OAK RIDGE NATIONAL LABORATORY LIBRARIES
3 4456 0570514 5

MARTIN MARIETTA

K/CSD/TM-58
Dist. Category UC-95c

COMPUTING AND TELECOMMUNICATIONS DIVISION

THE USE OF ROOF TEMPERATURE MODELING TO PREDICT NECESSARY CONDITIONS FOR LOCATING WET INSULATION WITH INFRARED THERMOGRAPHY

K. W. Childs

OPERATED BY
MARTIN MARIETTA ENERGY SYSTEMS, INC.
FOR THE UNITED STATES
DEPARTMENT OF ENERGY

Printed in the United States of America. Available from
National Technical Information Service
U.S. Department of Commerce
5285 Port Royal Road, Springfield, Virginia 22161
NTIS price codes—Printed Copy: A03 Microfiche A01

This report was prepared as an account of work sponsored by an agency of the United States Government. Neither the United States Government nor any agency thereof, nor any of their employees, makes any warranty, express or implied, or assumes any legal liability or responsibility for the accuracy, completeness, or usefulness of any information, apparatus, product, or process disclosed, or represents that its use would not infringe privately owned rights. Reference herein to any specific commercial product, process, or service by trade name, trademark, manufacturer, or otherwise, does not necessarily constitute or imply its endorsement, recommendation, or favoring by the United States Government or any agency thereof. The views and opinions of authors expressed herein do not necessarily state or reflect those of the United States Government or any agency thereof.

K/CSD/TM-58
Dist. Category UC-95c

THE USE OF ROOF TEMPERATURE MODELING TO PREDICT NECESSARY CONDITIONS FOR LOCATING WET INSULATION WITH INFRARED THERMOGRAPHY

K. W. Childs
Technical Applications

Date of Issue: November 1985

COMPUTING AND TELECOMMUNICATIONS DIVISION
at
Oak Ridge Gaseous Diffusion Plant
Post Office Box P
Oak Ridge, Tennessee 37831

Martin Marietta Energy Systems, Inc.
operating the
Oak Ridge Gaseous Diffusion Plant Oak Ridge National Laboratory
Oak Ridge Y-12 Plant Paducah Gaseous Diffusion Plant
under contract No. DE-AC05-84OR21400
for the
Department of Energy

CONTENTS

	PAGE
LIST OF FIGURES	vii
ABSTRACT	1
INTRODUCTION	1
ANALYTICAL MODEL	2
INSULATION PROPERTIES	4
CALORIMETRIC SKY TEMPERATURE	7
INSOLATION AND SOLAR ABSORPTANCE	7
OUTDOOR TEMPERATURE	10
WIND	15
OTHER PARAMETERS	15
MODEL VERIFICATION	15
DEVELOPMENT OF SIMPLE MODEL	19
INFLUENCE OF OTHER FACTORS	32
CONCLUSIONS AND RECOMMENDATIONS	40
ACKNOWLEDGMENTS	41
REFERENCES	43

LIST OF FIGURES

FIGURE		PAGE
1.	Roof system modeled	5
2.	Change in thermal properties of fibrous glass insulation with moisture	6
3.	Calorimetric sky temperature	8
4.	Surface ΔT resulting from a constant air temperature and from the same constant temperature plus insolation	9
5.	Influence of solar absorptance on roof surface temperature for a sunny winter day	11
6.	Surface ΔT resulting from different solar absorptance	12
7.	Outdoor air temperature cycles used to examine dynamic effect due to temperature swing	13
8.	Surface ΔT resulting from temperature cycles of Fig. 7	14
9.	Roof temperatures - March 28-31, 1984	17
10.	Roof temperatures - April 3-9, 1984	18
11.	Effect of outdoor air temperature on surface ΔT	20
12.	Effect of diurnal temperature swing on surface ΔT	21
13.	Effect of insolation on surface ΔT	22
14.	Effect of wind on surface ΔT	23
15.	Coefficients for simple model - case 1	26
16.	Coefficients for simple model - case 2	27
17.	Coefficients for simple model - case 3	28
18.	Coefficients for simple model - case 4	29
19.	Coefficients for simple model - case 5	30
20.	Coefficients for simple model - case 6	31
21.	Comparison of simple model and computer model results	33
22.	Coefficients for simple model - case 7	34
23.	Coefficients for simple model - case 8	36
24.	Effect of moisture location on wet/dry temperature difference	37
25.	Effect of gravel weight on wet/dry temperature difference	38
26.	Effect of viewing time on wet/dry temperature difference	39

THE USE OF ROOF TEMPERATURE MODELING TO PREDICT NECESSARY CONDITIONS FOR LOCATING WET INSULATION WITH INFRARED THERMOGRAPHY

K. W. Childs

ABSTRACT

In low-sloped roofing systems using porous insulation, the presence of water can significantly degrade thermal performance. For this reason, it is desirable to develop a reliable method for detecting the presence of water in a roofing system. Because of the different thermal characteristics of wet and dry insulation, there is often a surface temperature differential between areas containing wet insulation and areas containing dry insulation. Under the right circumstances, the areas of wet insulation can be detected by means of infrared sensing techniques. These techniques have already gained widespread acceptance, but there is still some uncertainty as to what are appropriate environmental conditions for viewing.

To better define the conditions under which infrared techniques can distinguish between areas of wet and dry insulation, a one-dimensional, transient heat transfer model of a roofing system was developed. The model considers conduction through the roof, insolation on the surface, radiant exchange between the roof and sky, convective heat transfer between the roof and air, and the influence of trapped moisture on the thermal properties of the insulation. A study was undertaken using this model to develop an easily-applied technique for prediction of necessary conditions for locating wet roof insulation using infrared thermography.

INTRODUCTION

Roof moisture surveys using infrared imaging devices have become fairly routine. A successful survey depends on the roof system and environmental conditions being such that wet areas can be distinguished from dry areas on the basis of surface temperature. The purpose of this report is to develop a technique for predicting, on the basis of specific roof characteristics and environmental conditions, differences in the roof surface temperature over areas containing dry insulation and over areas containing moist insulation. This capability will allow someone conducting a roof moisture survey to decide whether environmental conditions are favorable for definitive viewing.

The roofs of interest in this study are low-pitched roofs of the type commonly used in commercial buildings. They are made up of three primary components: (1) the deck, which is part of the structural system and supports the roof; (2) the insulation, which provides a thermal barrier to heat flow; and (3) the weatherproofing, which protects the insulation and building from water penetration. There is often a layer of gravel placed on top of the roof to protect the weatherproofing from ultraviolet radiation. Although the deck, weatherproofing, and gravel contribute some resistance to heat flow, it is the insulation which provides the predominant resistance in a dry roof. Water alters the properties of insulation, and thus can have a marked effect on the thermal behavior of the entire roof system.

There are two heat transfer phenomena which can produce a surface temperature difference between the portion of a roof containing wet insulation and the portion containing dry insulation.

These phenomena result from the influence of moisture on the thermophysical properties of the insulation. The first of these is due to the reduced R-value (increased conductivity) of wet insulation as compared to dry insulation. This manifests itself most strongly during cold weather when greater heat loss through the wet insulation results in a warmer roof surface temperature above the wet insulation than above dry insulation. This effect diminishes as the outdoor temperature rises and will reverse itself (i.e., wet areas will be cooler than dry areas) when the outdoor temperature is higher than the indoor temperature.

There have been several mathematical roof models developed[1,2,3] that predict what weather conditions are necessary to produce a temperature difference between roofs of different R-value observable with infrared thermography. None of the studies were aimed specifically at different R-values resulting from the presence of moisture, but they could be used for this purpose. Their major drawbacks are that they assume steady-state conditions and focus on cold weather effects only.

The second phenomenon results from the increased heat storage capacity of wet insulation as compared to dry insulation. Knehans and Styer[4], Korhonen and Tobiasson[5], Fishburn[6], and Tobiasson[7] have all recognized that the additional heat storage in wet insulation contributes to the temperature difference between areas of wet and dry insulation during warm weather. However, these authors do not quantify the magnitude of this temperature difference. This is a dynamic effect, and the previously-mentioned steady-state models do not address it. There are two driving forces that produce this effect: absorption of solar radiation (insolation) and the daily swing in the outdoor temperature (diurnal swing). During the daytime, both a dry and wet portion of a roof will heat up due to higher daytime temperature and insolation on the roof surface. Because of the added heat capacity of the water, the wet areas will rise in temperature more slowly than the dry areas. However, the wet areas will actually store more energy than the dry areas. At night when the outside temperature drops and insolation is no longer a factor, the roof will lose energy to the surroundings and drop in temperature. The dry areas will cool rapidly because there is relatively little energy stored in the dry insulation, while the temperature of the wet areas will fall more slowly because of the additional stored energy. The net effect of this is that the roof surface temperature over an area with wet insulation will be cooler during the day and warmer at night than the roof surface temperature over areas of dry insulation.

These two phenomena are not mutually exclusive. Both are always present to some degree. Sometimes they are additive; sometimes they tend to cancel each other out; sometimes one effect will dominate; but both effects need to be considered in any model used to predict roof surface temperatures.

Emphasis in this analysis is placed on predicting the effect of different parameters on the roof surface temperature difference over areas of wet and dry insulation. As used in this report, ΔT refers to the roof surface temperature difference between areas of wet and dry insulation ($\Delta T = T_{wet} - T_{dry}$). While changes in temperature difference are not as readily intuitive as changes in surface temperature, it does have the advantage of being directly useful in infrared studies. A typical infrared thermographic image will show a roof section which is part wet and part dry in terms of differences in radiosity between wet and dry areas. This difference in radiosity is directly relatable to a difference in surface temperature. Thus it is appropriate to express results in these terms.

ANALYTICAL MODEL

Determination of the roof surface temperature requires solution of a one-dimensional conduction heat transfer problem in a system made up of layers of materials with different properties. At the

upper surface of the roof, the heat conducted into or out of the roof at any time must be equal to the net heat flow to the roof produced by the combined effects of solar gain, convection, and radiative exchange with the sky. That is

$$q\Big|_{upper\ surface} = -k\frac{\partial T}{\partial x}\Big|_{upper\ surface} \tag{1}$$

$$= \alpha q_{solar} - h_u\left(T_s - T_{air}\right) - \epsilon\sigma\left(T_s^4 - T_{sky}^4\right) ,$$

where

k	=	thermal conductivity at material at upper surface of roof,
α	=	solar absorptivity of the roof surface,
q_{solar}	=	rate of solar energy striking roof,
h_u	=	convective heat transfer coefficient,
ϵ	=	emittance of roof surface in infrared,
σ	=	Stefan-Boltzmann constant,
T	=	roof temperature,
T_{sky}	=	calorimetric sky temperature,
T_s	=	surface temperature (the unknown of primary interest),
T_{air}	=	outside air temperature.

At the lower surface of the roof, the heat transfer is assumed to be entirely by convection. That is

$$q\Big|_{lower\ surface} = -k\frac{\partial T}{\delta x}\Big|_{lower\ surface} = h_l\left(T_s - T_{air}\right) , \tag{2}$$

where

k	=	thermal conductivity of material at lower surface of roof,
h_l	=	convective heat transfer coefficient (inner surface),
T	=	roof temperature,
T_s	=	inside surface temperature,
T_{air}	=	inside air temperature.

It is not possible to obtain a general, closed-form solution for this problem. However, there are several numerical methods by which the solution for any particular case can be obtained. These

include finite difference, finite element, and response factor methods. Both finite difference and finite element require that the entire temperature field through the roof be solved in order to obtain the surface temperature. In this problem, the temperature distribution is not required; thus, using either of these methods with their relatively long computer run time is not justified.

The response-factor method does not entail the determination of the entire temperature field and is consequently much faster. However, the response-factor method is applicable only to linear problems. If the assumption is made that the properties of the materials making up the roof are not temperature dependent, the conduction within the roof becomes linear. The boundary condition on the lower surface of the roof is also linear, but the boundary condition on the upper surface is not linear in temperature due to the radiation terms. Application of the response-factor method to the linear portion of the problem results in a linear algebraic equation which gives the heat flux at the upper surface of the roof as a function of the current and prior upper roof surface temperature and inside air temperature. The coefficients in this equation are a function of the number, thickness, and material properties of the layers making up the roof system and only need to be determined once for any particular roof system.

Equation 1 gives the current heat flux at the upper surface of the roof as a function of the current surface temperature and current environmental conditions. The determination of the current surface temperature requires only the solution of these two equations in two unknowns (upper surface temperature and heat flux). However, the prior history of the surface temperature is required to begin the calculation. Since this is not known, a history must be assumed and the calculations continued for a long enough period of time so that the assumed history no longer influences the results. To determine the temperature difference between areas of wet and dry insulation, the surface temperature is calculated twice: once with the properties of dry insulation and once with the insulation properties altered to account for the effects of moisture.

The parameters appearing in the model include: (1) the roof material properties for each layer, (2) the inside air temperature and heat transfer coefficient, (3) the external weather conditions (insolation, air temperature, sky temperature), and (4) the roof surface infrared emittance and solar absorptance. Parameters that do not appear explicitly in the equations are the wind speed, which appears indirectly in the external convective heat transfer coefficient, and the influence of moisture, which appears as a change in the thermal properties of the insulation.

To determine the importance of these parameters, the particular roof shown in Fig. 1 was employed. This roof has a 3-inch thick concrete deck, a 1-inch nominal thickness glass fiber insulation board, a weatherproofing membrane, and a gravel topping. The various parameters are discussed in the following sections.

INSULATION PROPERTIES

The presence of moisture increases the conductivity (decreases the R-value) of the insulation. A plot of thermal conductivity versus moisture content for a fibrous glass insulation is presented in Fig. 2. This is based on the experimental data of Korhonen and Tobiasson.[5] The presence of moisture also increases the mass, and thus the heat storage capacity of insulation. The heat capacity per-unit-volume of insulation can be calculated as

$$C = \left(\rho c_p\right)_{dry\ insulation} + \frac{X}{100}\left(\rho c_p\right)_{water} , \qquad (3)$$

ORNL-DWG 83-7423

ROOF SYSTEM MODELED

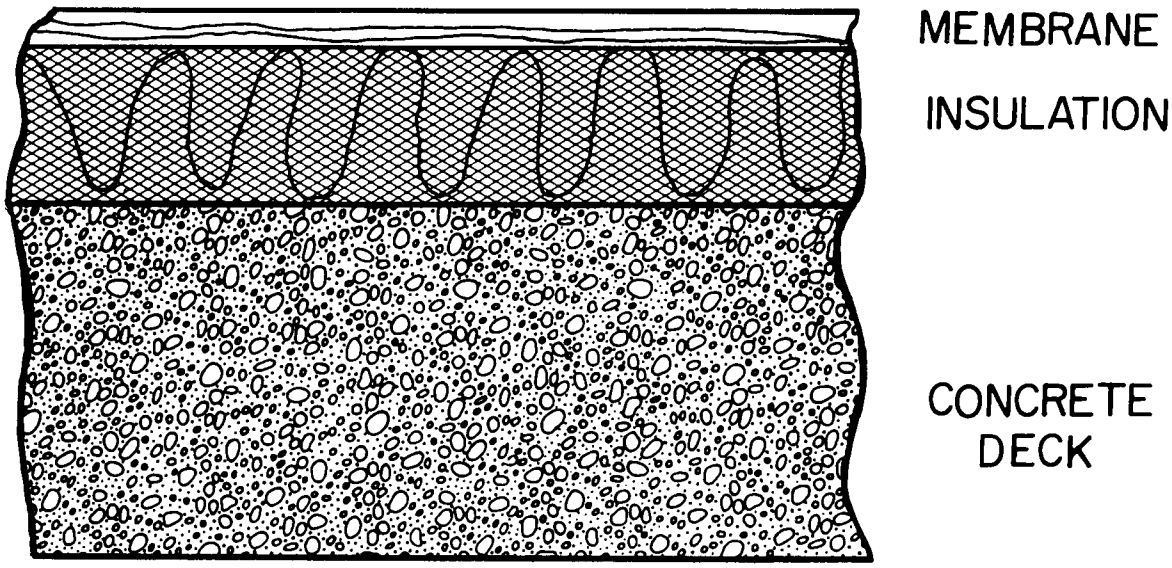

Fig. 1. Roof system modeled.

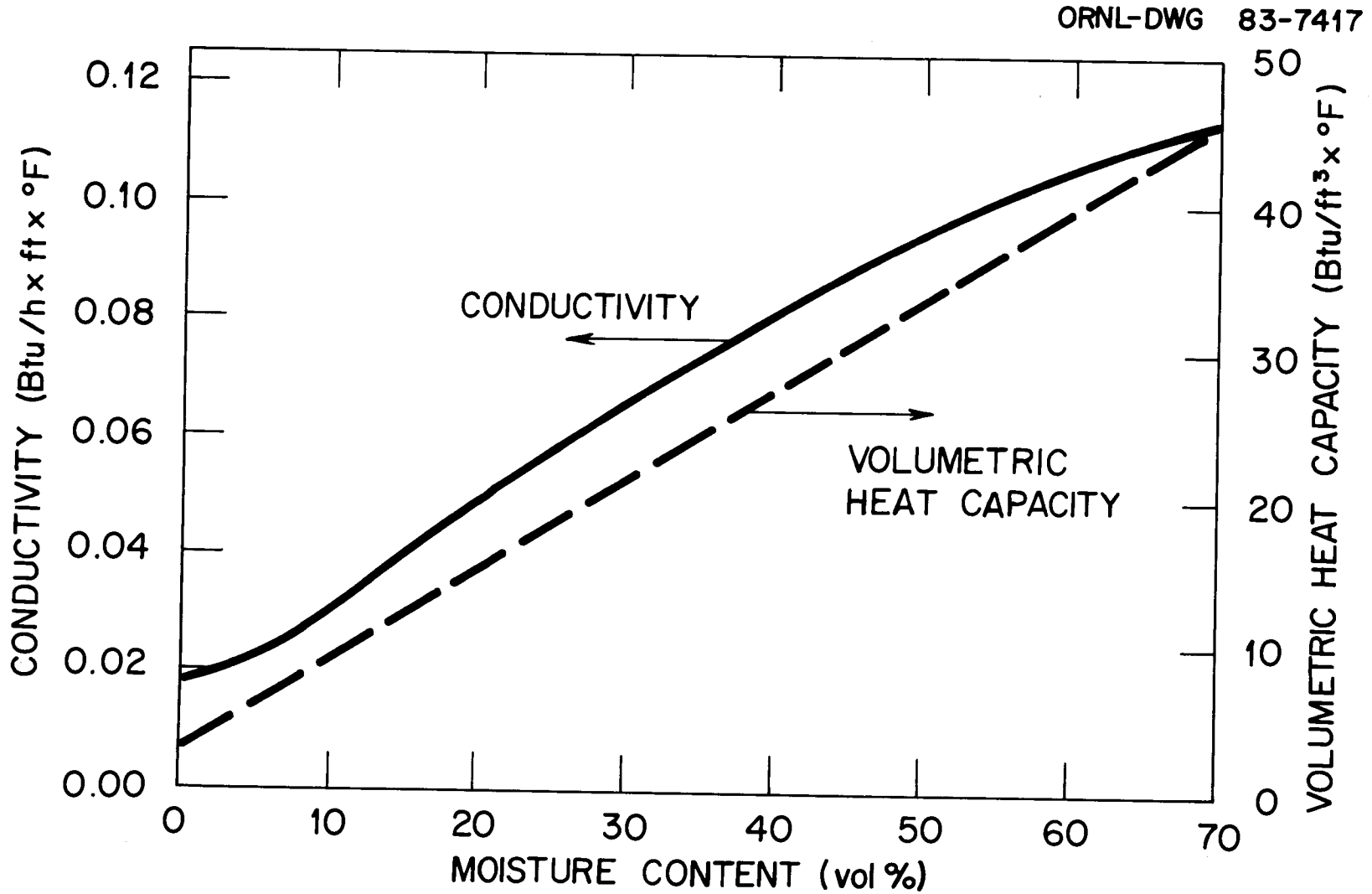

Fig. 2. Change in thermal properties of fibrous glass insulation with moisture.

where

C = volumetric heat capacity,
ρ = density of either dry insulation or water,
c_p = specific heat of either dry insulation or water,
X = volume percent moisture content.

For most of this analysis it is assumed that when moisture is present, it is uniformly distributed through the thickness of the insulation. There is one case presented that addresses the consequences of this assumption being violated. It is also assumed that the amount of moisture in the insulation is fixed, and that it does not migrate or change phases. The consequences of the moisture migrating or changing phases are beyond the scope of this study, but it is currently being investigated.

CALORIMETRIC SKY TEMPERATURE

An important parameter in the roof surface energy balance equation (Eq. 1) is the calorimetric sky temperature. The following correlation developed from work by Swinbank[8] has been widely used in modeling to give the effective calorimetric sky temperature for clear conditions

$$T_{sky} = 0.0412\ T_{air}^{1.5} \quad , \tag{4}$$

where T_{air} is the air temperature near the ground and T_{sky} is the calorimetric sky temperature (both are in °R). The sky temperature for totally overcast conditions is normally assumed to be equal to the air temperature.

Beginning in late spring of 1983, an infrared radiometer (pyrgeometer) to measure radiation on a horizontal surface from the sky in the infrared range was installed at an experimental facility at Oak Ridge National Laboratory (ORNL). The data were compared to the above correlations for sky temperature. The assumption that the sky temperature is equal to the air temperature for overcast conditions appears to be substantiated by the data. However, the data do not substantiate the Swinbank correlation. Other correlations have been developed by Bliss[9] and Goldstein[10] which incorporate humidity effects. Examination of the ORNL data also suggests that the sky temperature is dependent on the amount of moisture in the air. Thus, the humidity-dependent models appear to be more realistic. While data collected thus far do not cover a wide enough range of temperature and humidity to make any definite conclusions, the Goldstein correlation appears to give the best agreement. Figure 3 shows the relationship between the Swinbank and Goldstein correlations for various dewpoint temperatures.

In using the analytical model to calculate the roof surface temperature difference between areas of wet and dry insulation, it turns out that there is not much difference in the results obtained using either the Swinbank or Goldstein correlations. Thus, the Swinbank correlation will be used. This has the practical benefit of eliminating one variable (humidity) from the parametric study.

INSOLATION AND SOLAR ABSORPTANCE

As already mentioned, solar energy stored in the wet insulation during the day and released at night contributes to the roof surface temperature difference between wet and dry areas. Figure 4

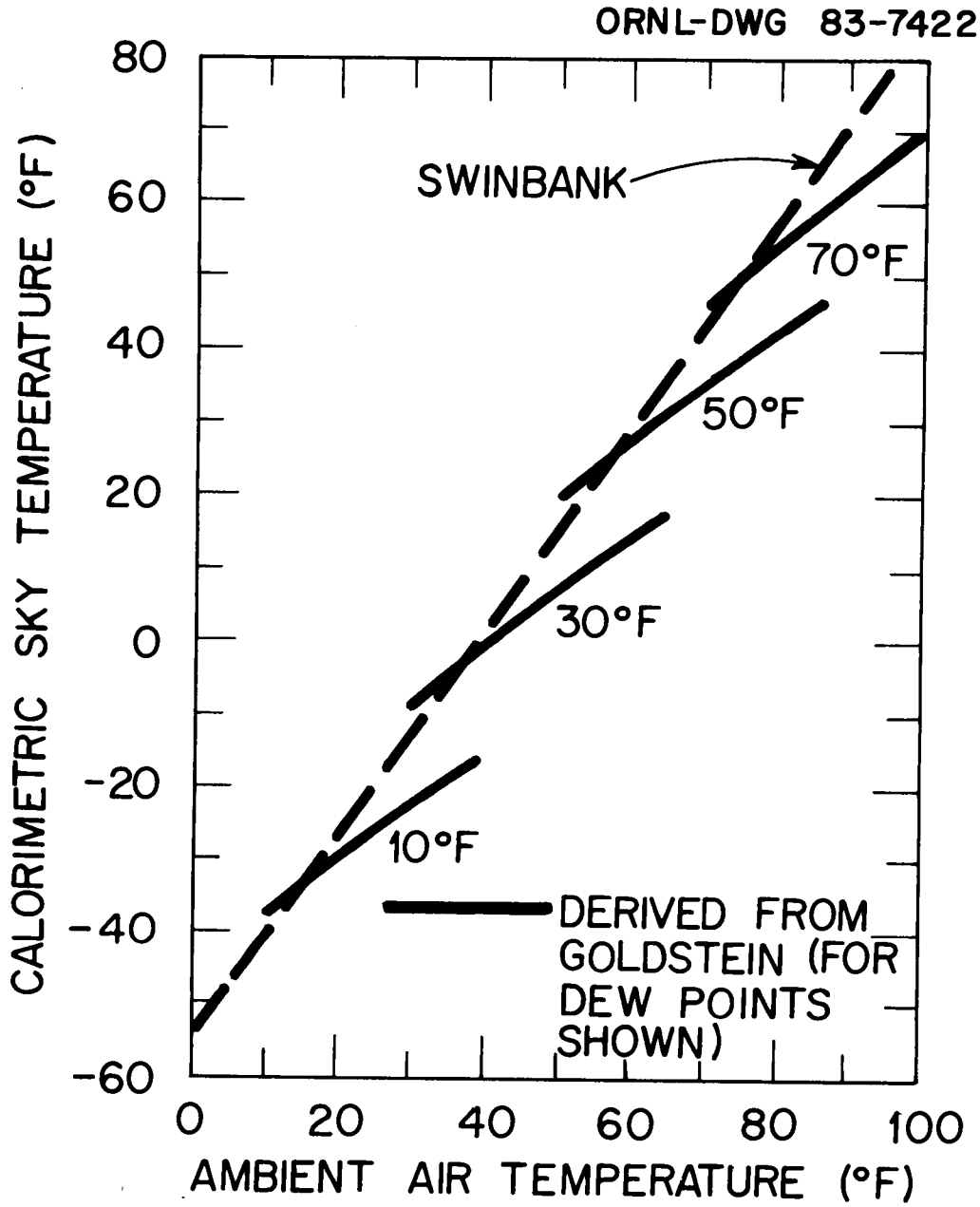

Fig. 3. Calorimetric sky temperature.

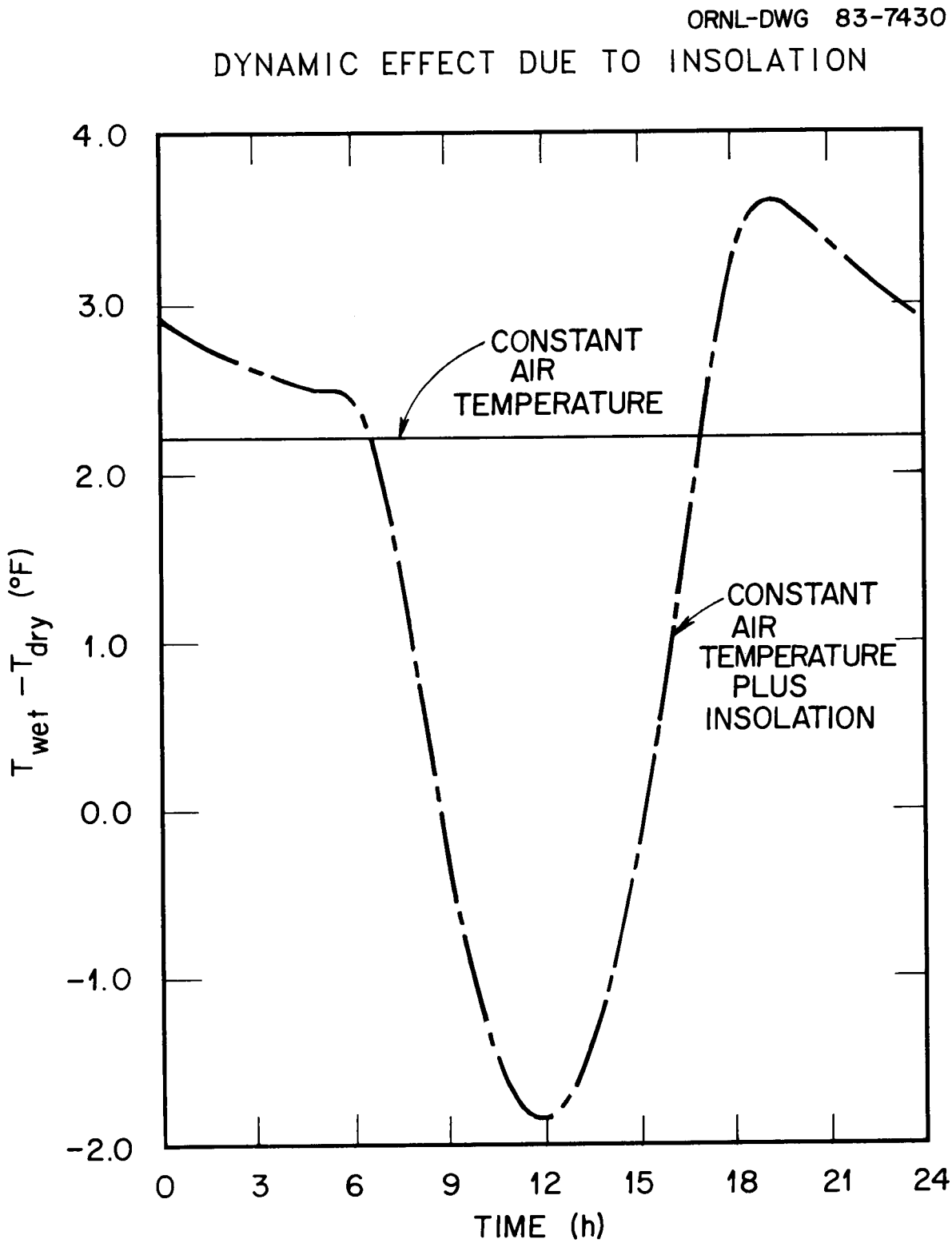

Fig. 4. Surface ΔT resulting from a constant air temperature and from the same constant temperature plus insolation.

shows the calculated temperature difference between areas of wet and dry insulation for two cases: one with and one without solar gain. Both cases assume that the wet area contains 60% moisture by volume and that indoor and outdoor temperatures are constant at 70°F and 45°F, respectively. In the absence of insolation and with constant inside-outside temperature difference, ΔT is determined solely by this inside-outside temperature difference and is a constant 2.2°F. The effect of insolation (with inside-outside temperature difference held constant) is shown by the oscillating curve. The sun obviously has an effect even at night, producing a larger temperature difference than would be calculated neglecting the solar effect. Note that the temperature difference has a maximum positive value shortly after sundown and decreases throughout the night.

The above calculation has assumed that the solar absorptance, hence the amount of energy absorbed, is the same over the entire roof. This, unfortunately, is often not the case. Because of staining of the roof or other causes, the solar absorptance may be different over areas of wet and dry insulation.

To evaluate the potential impact of differing solar absorptances, the surface temperature was calculated for four cases: a dry roof with an absorptance of 0.4 and three wet roofs with absorptances of 0.4, 0.5 and 0.6. The calculated roof surface temperature for sunny, winter conditions are presented in Fig. 5. Figure 6 gives the values of ΔT for the same conditions.

When both the wet and dry areas have the same absorptance, the behavior is as anticipated: the wet area is cooler than the dry area in the daytime and warmer at night. However, as the absorptance of the wet area increases, the daytime behavior is altered significantly. The wet area is no longer necessarily cooler in the daytime, and, in fact, can be substantially warmer. Without some knowledge of the absorptance, it is no longer possible to distinguish between wet and dry areas on the basis of surface temperature. However, the nighttime behavior is virtually unchanged. Therefore, if differences in absorptance exist across a roof surface, the use of thermography to detect areas of wet insulation can best be accomplished at night. Daytime observations may be ambiguous. Additional runs for summer conditions produced the same conclusions.

OUTDOOR TEMPERATURE

In most previous calculations of roof surface temperature, the instantaneous air temperature and a steady-state equation have been used. Because of dynamic effects, this can give misleading information. To illustrate this effect, consider the two temperature histories given in Fig. 7. One is simply a constant air temperature of 45°F. The other is a sinusoidally varying air temperature with an average of 60°F and a variation of ±15°F. At three o'clock in the morning, the outside air temperatures are the same for both cases, but at all other times the sinusoidally varying temperature is higher than the constant temperature. Figure 8 presents the calculated ΔT for both cases. At three o'clock in the morning, this temperature difference is substantially larger for the sinusoidally varying temperature than for the constant temperature, even though the instantaneous air temperatures are the same. Thus, the instantaneous temperature is not a good indicator of ΔT. A better choice of parameters is average outdoor temperature and diurnal temperature swing. The maximum temperature difference does occur at the time of minimum outdoor temperature.

Another interesting aspect of this example is that the indoor/outdoor air temperature difference is always less for the sinusoidally varying outdoor temperature than for the constant outdoor temperature. Yet, because of dynamic effects, the wet/dry surface temperature difference is greater for the sinusoidal case from 10 p.m. to 7 a.m. Thus, better infrared viewing conditions may exist when there has been a large outdoor temperature swing than when the outdoor temperature has been colder, but with less variation.

ORNL-DWG 83-7433

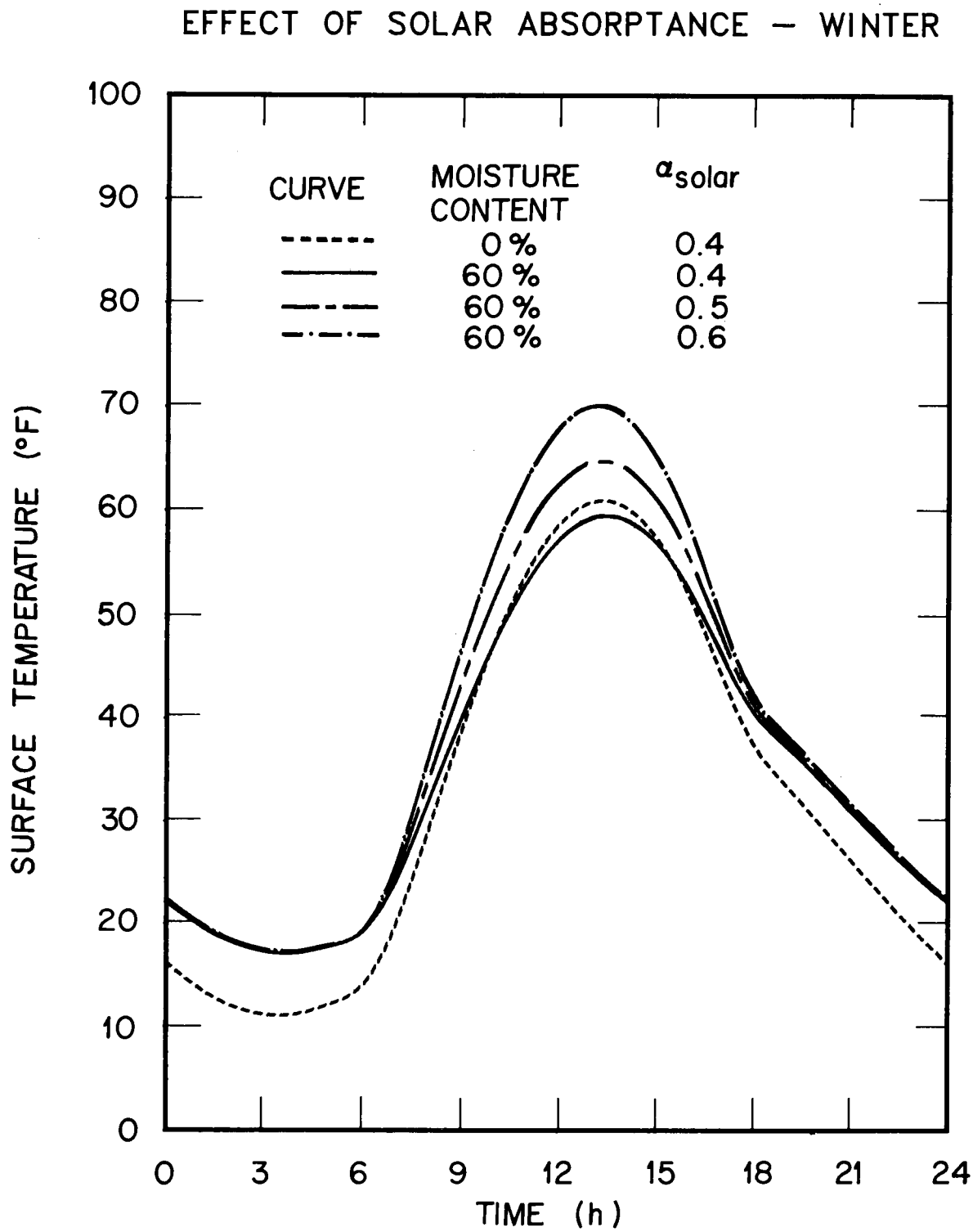

Fig. 5. Influence of solar absorptance on roof surface temperature for a sunny winter day.

ORNL-DWG 83-7432

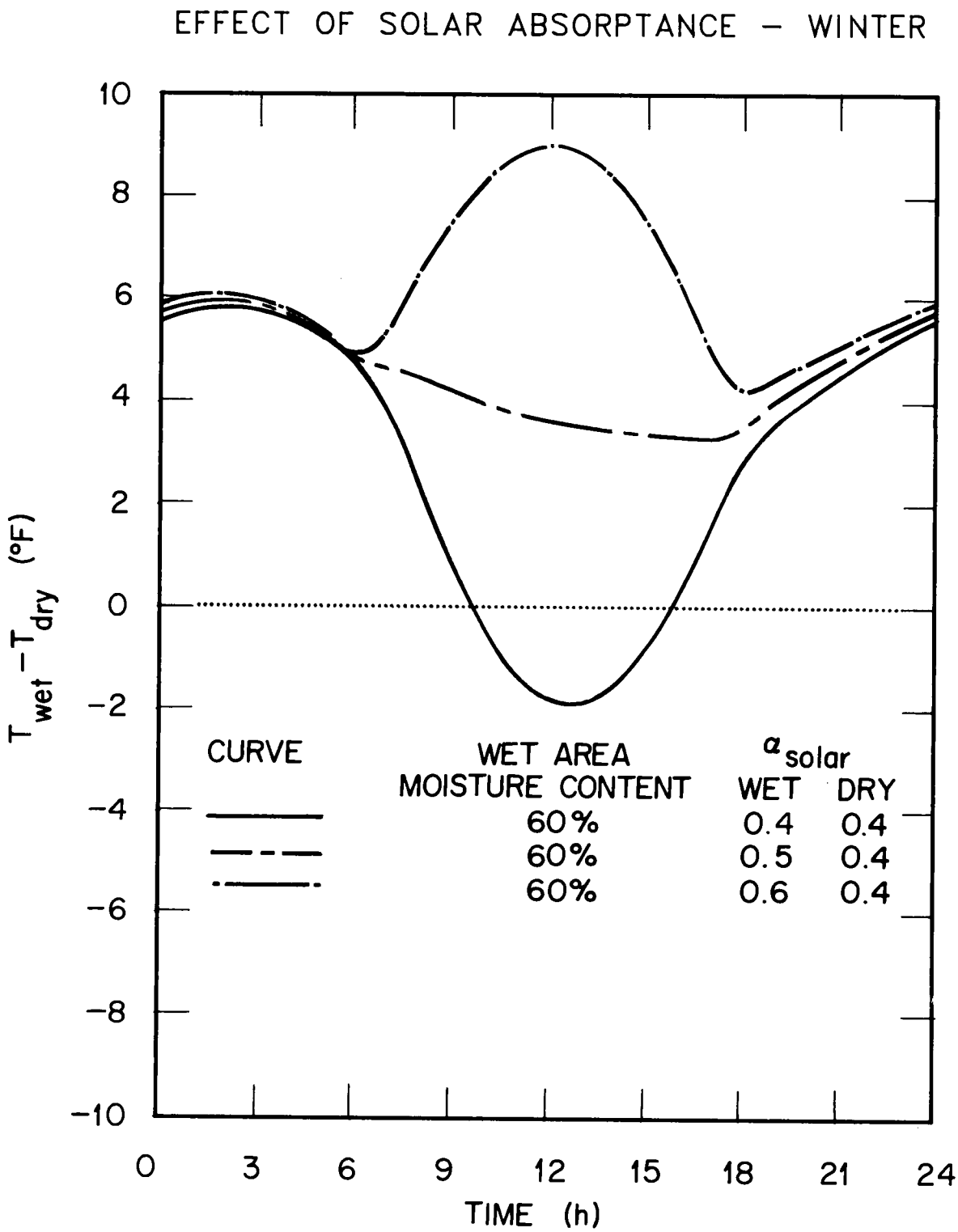

Fig. 6. Surface ΔT resulting from different solar absorptance.

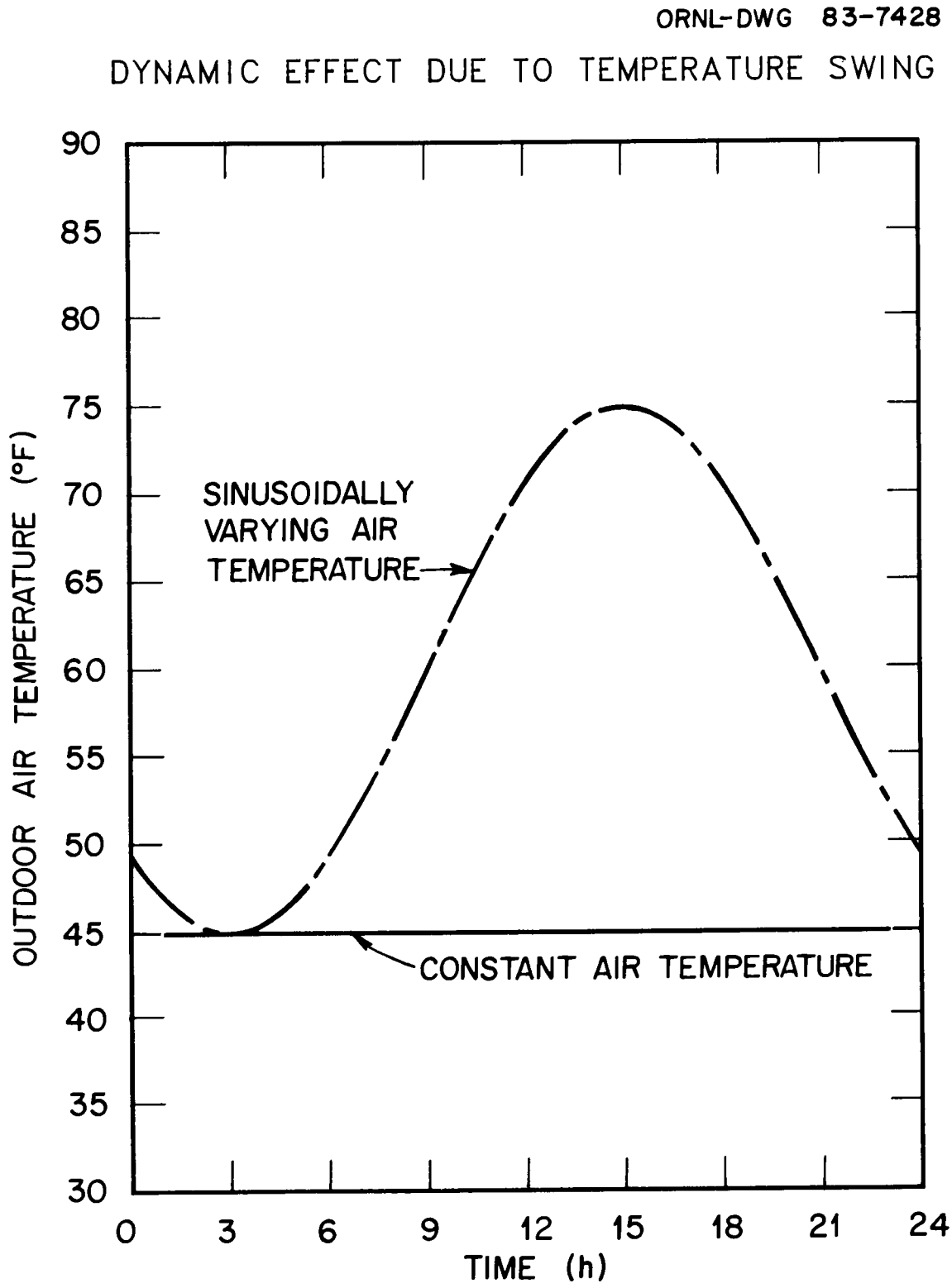

Fig. 7. Outdoor air temperature cycles used to examine dynamics effect due to temperature swing.

ORNL-DWG 83-7429

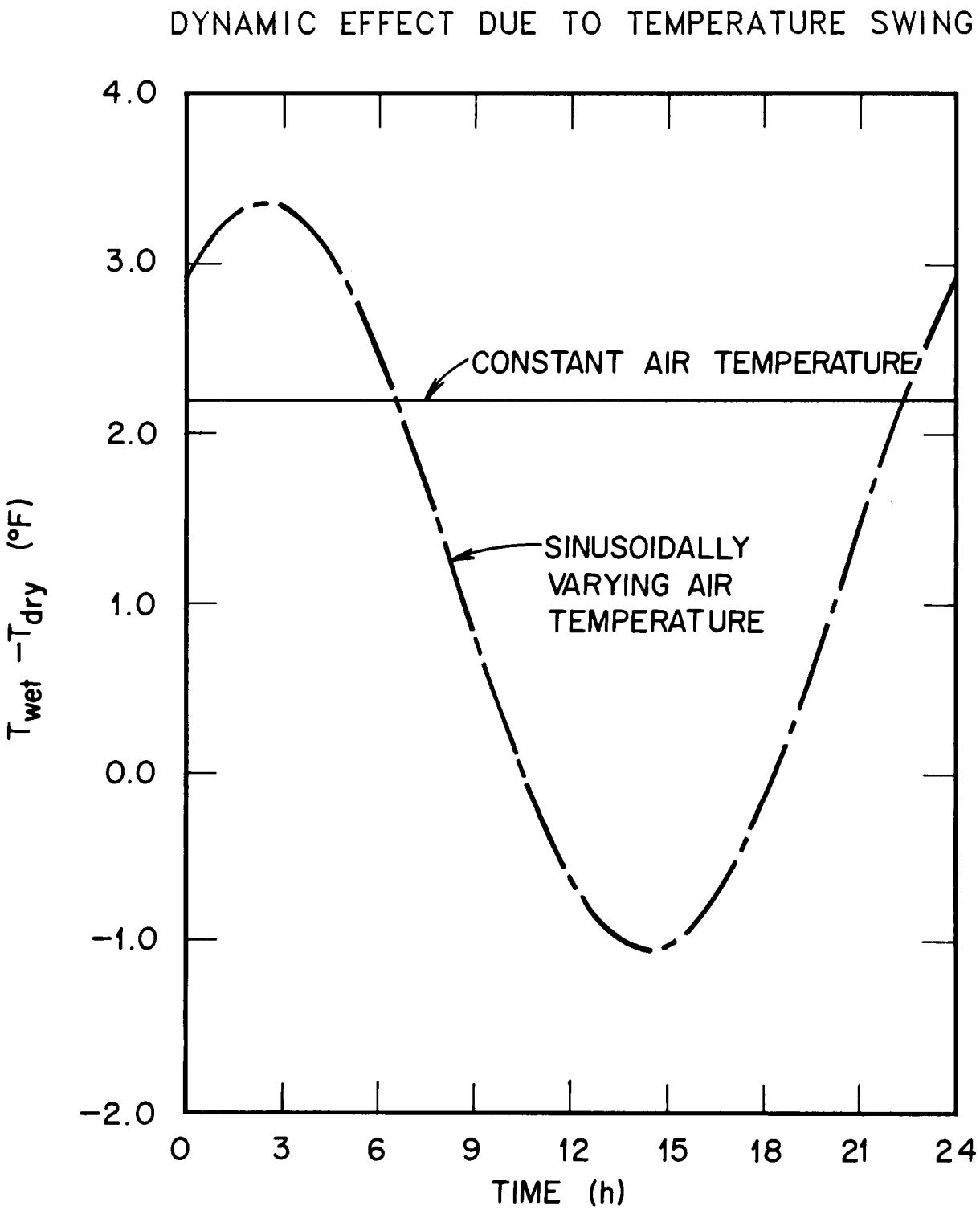

Fig. 8. Surface ΔT resulting from temperature cycles of Fig. 7.

WIND

The wind obviously is an important parameter in determining the roof surface temperature. As the wind speed increases, the surface heat transfer coefficient increases, and the surface/air temperature difference required to transfer a given amount of heat decreases. Thus, even though there may be a substantial difference in heat transfer between areas of wet and dry insulation, this will not result in large temperature differences under windy conditions. The convective heat transfer coefficient used in the model is obtained from Ref. 11 and is given by

$$h = 0.29V + 0.95 \quad , \tag{5}$$

where V is the wind speed in mph and h is in Btu/hr·ft^{2}·°F.

OTHER PARAMETERS

For the purposes of this study the inside air temperature will be fixed at a typical 70°F for all cases. The results presented in this report are primarily for one particular insulation type, glass fiberboard. Moisture levels of 30% and 60% by volume will be considered. The infrared emittance of the roof is assumed to be constant with a value of 0.9, since the emittance of most roofing materials varies over a very small range near this value.

MODEL VERIFICATION

In order to determine if roof surface temperatures can be accurately predicted with a numerical model such as just described, a comparison was made between predictions from the model and measured surface temperatures from the Roof Thermal Research Apparatus (RTRA) Facility at Oak Ridge National Laboratory. This facility has the capability of simultaneously testing four different roof panels, each measuring 4 by 8 ft. The panels are instrumented to measure the roof surface temperatures as well as the temperature distribution through the roof, and the heat flux at the inside surface. A comprehensive weather station is located at the facility to measure environmental conditions. Each panel is mounted on load cells so that its weight can be accurately determined, which allows the determination of the amount of water in a panel. A direct side-by-side comparison can be made of a panel with dry insulation and a panel with a known amount of water present. At the time this report was being prepared, the RTRA facility was not fully operational. Instrumentation was installed on only one test panel to check out the data acquisition system. This check-out panel had a steel deck, 2 in. of glass fiberboard insulation, and a built-up roof of felt and asphalt. There was no water in this roof test panel.

Since the available data were obtained during the start-up and check-out phases of the test facility, it was difficult to obtain long stretches of uninterrupted data. However, two stretches of data of sufficient length to check the model were obtained: a 4-day period (March 28-31, 1984)

and a 7-day period (April 3-9, 1984). In testing the model, a calorimetric sky temperature (obtained from the long-wave sky radiation data measured at the weather station) was used. The Swinbank correlation was not used because it is for clear sky conditions, which were not present during much of the test period. In the preliminary comparisons of measured and calculated roof surface temperature, it appeared that the wind speed had a greater influence on the calculated temperature than was observed in the measured value. It was speculated (and later verified by measurement) that the wind speed measured at a height of approximately 6 ft above the roof test panel might not be representative of the wind at the surface. This was accounted for in subsequent calculations by altering Eq. 5 so that the heat transfer coefficient was less dependent on the "measured" wind speed. This is given in Eq. 5.′

$$h = 0.145V + 0.95 \tag{5'}$$

This alteration was not incorporated as a permanent change in the model but was done only for this comparison. The calculated and measured surface temperatures for the two periods are given in Figs. 9 and 10. Also presented in these figures are the air temperature and calorimetric sky temperature. In both figures the first 24-hour period should not be used to compare the measured and calculated surface temperatures since the prior temperature history required in the calculations was not known, and an assumed history had to be used. The history was arrived at by assuming that the days immediately prior to the beginning of data collection were identical to the first 24 hours of data collected. The comparison of measured and calculated surface temperatures shows quite good agreement in both behavior and actual temperatures for the most part. The relatively large differences in the daytime peak temperatures occurring on days 95 and 97 appear to be related to the wind. On both of these days there were gusty winds in excess of 10 mph.

It is not yet possible to test the model on a roof containing wet insulation, but this will be done when there are more data available from the RTRA facility.

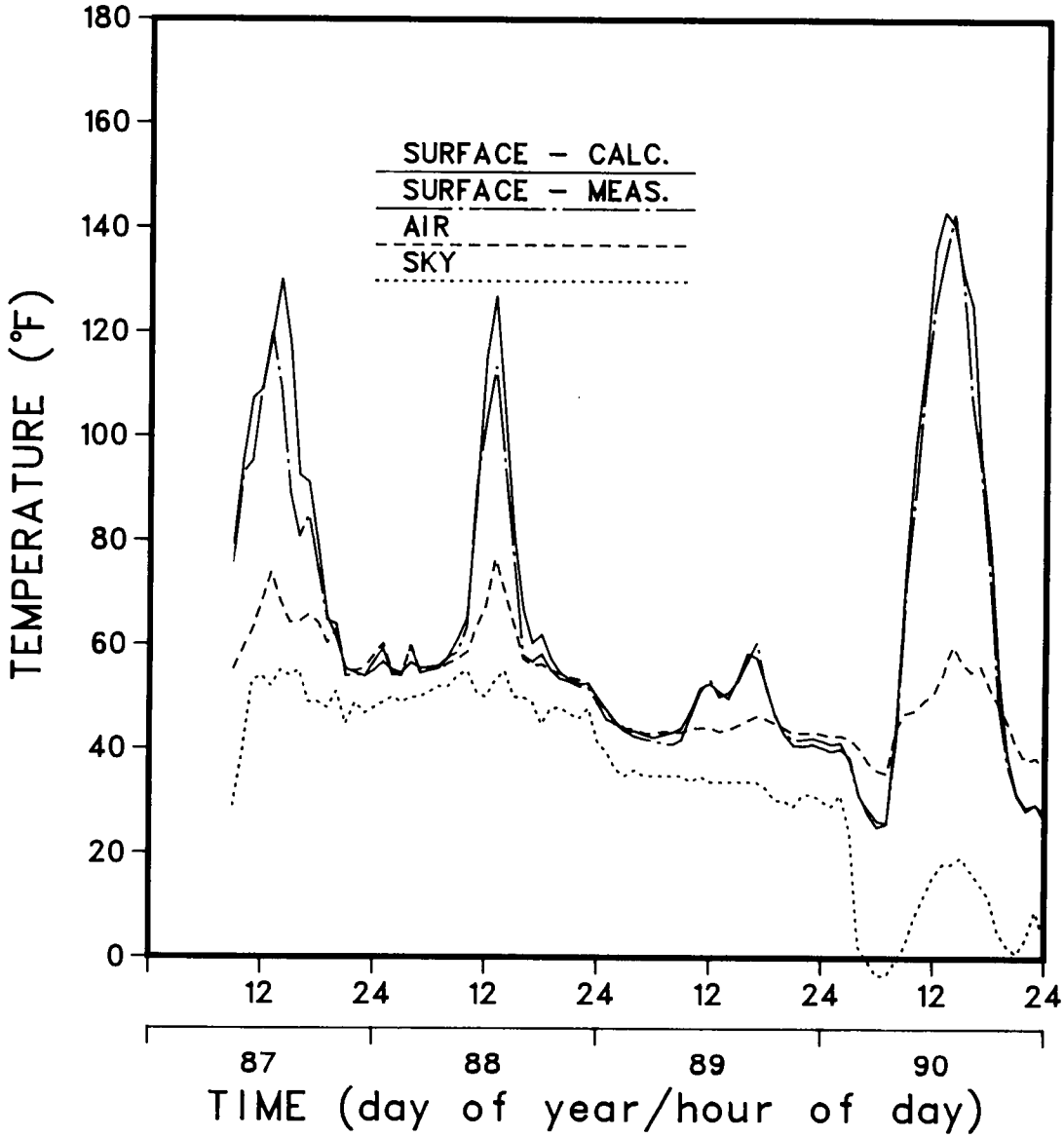

Fig. 9. Roof temperatures - March 28-31, 1984.

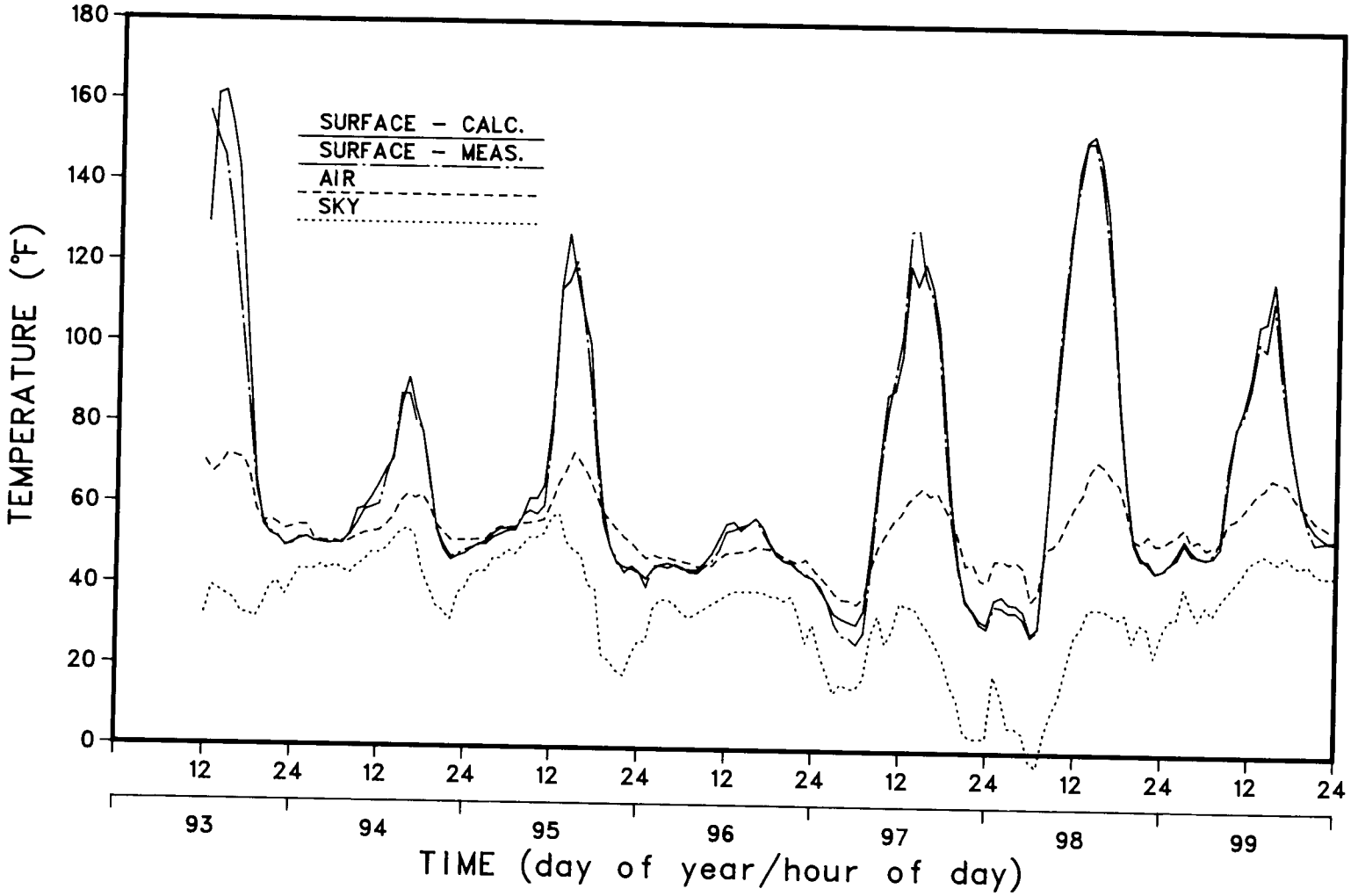

Fig 10. Roof temperatures - April 3-9, 1984.

DEVELOPMENT OF SIMPLE MODEL

When a closed-form analytical solution can be obtained, the influence of parameters can be readily determined either by simple observations of the forms of the equation or by differentiation with respect to a particular parameter of interest. However, when the only solution which can be obtained is by numerical means, such as in this case, the influence of the parameters cannot be as readily determined. In this situation, one must resort to a parametric study in which each parameter is varied either individually or in conjunction with other parameters with any changes in the result observed.

The parameters of primary interest are (1) average outdoor temperature, (2) diurnal temperature swing, (3) insolation, (4) wind, (5) sky conditions (clear or overcast), (6) insulation moisture content, and (7) the insulation level. The relative importance of all of the parameters on the surface temperature difference between areas of wet and dry insulation was determined for one particular roof. To accomplish this, a parameteric study was undertaken in which the outdoor temperature, diurnal temperature swing, insolation level, and wind speed were each individually varied over a range of values while the other three were fixed at a nominal value. This was done for two moisture levels (30% and 60%) and for two sky conditions (clear and overcast). The results are presented in Figs. 11 through 14 for the effects at midnight caused by each parameter. Midnight was chosen because of a need to reduce the amount of data to manageable proportions and because it is a common viewing hour for infrared operators. In Fig. 11, the influence of average outdoor temperature is given for different moisture contents and sky conditions. Similar curves for the influence of diurnal temperature swings and insolation are given in Figs. 12 and 13. In Fig. 12, the diurnal temperature swing is the difference between the maximum and minimum outdoor temperature for the 24-hour period. In Fig. 13, the insolation value must be adjusted for atmospheric condition. In Fig. 14, the effect of wind is given as the ratio of the temperature difference between areas of wet and dry insulation for windy conditions to that for no wind conditions. The moisture level did not have a significant influence, so the two curves presented (one for clear sky and one for overcast) are applicable to any moisture level.

Examination of the results of the parametric study suggested the format in which they are presented in Figs. 11 through 14. The total temperature difference between areas of wet and dry insulation can be estimated as

$$\Delta T = \left\{ \Delta T_{OT} + \Delta T_{DTS} + \Delta T_{I} \right\} \frac{\Delta T_{wind}}{\Delta T_{no\ wind}} , \tag{6}$$

where

ΔT	=	estimated temperature between wet and dry areas,
ΔT_{OT}	=	temperature difference due to average outdoor temperature (Fig. 11),
ΔT_{DTS}	=	temperature difference due to diurnal outdoor temperature swing (Fig. 12),
ΔT_{I}	=	temperature difference due to insolation (Fig. 13),
$\frac{\Delta T_{wind}}{\Delta T_{no\ wind}}$	=	ratio from Fig. 14.

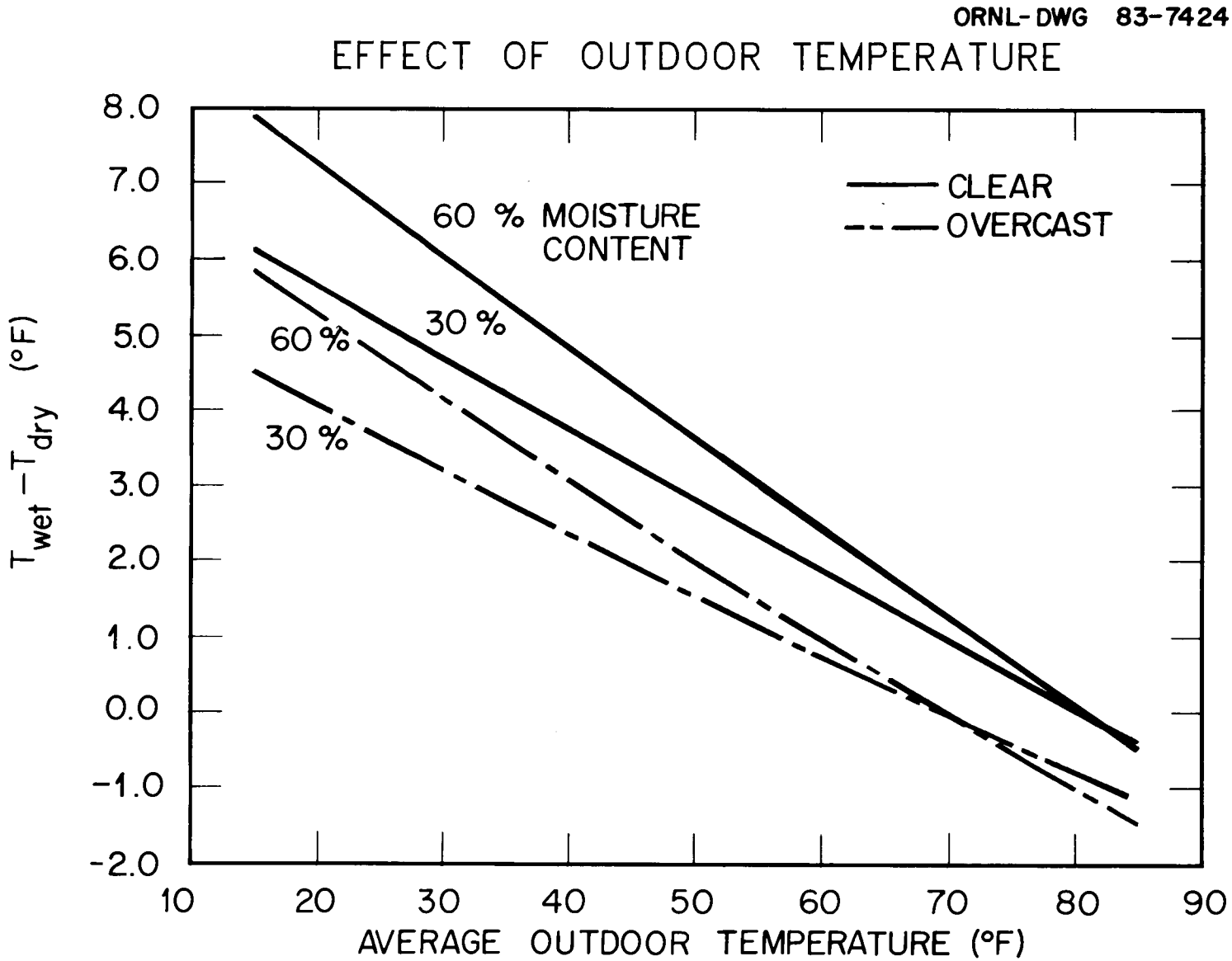

Fig. 11. Effect of outdoor air temperature on surface ΔT.

ORNL-DWG 83-7426

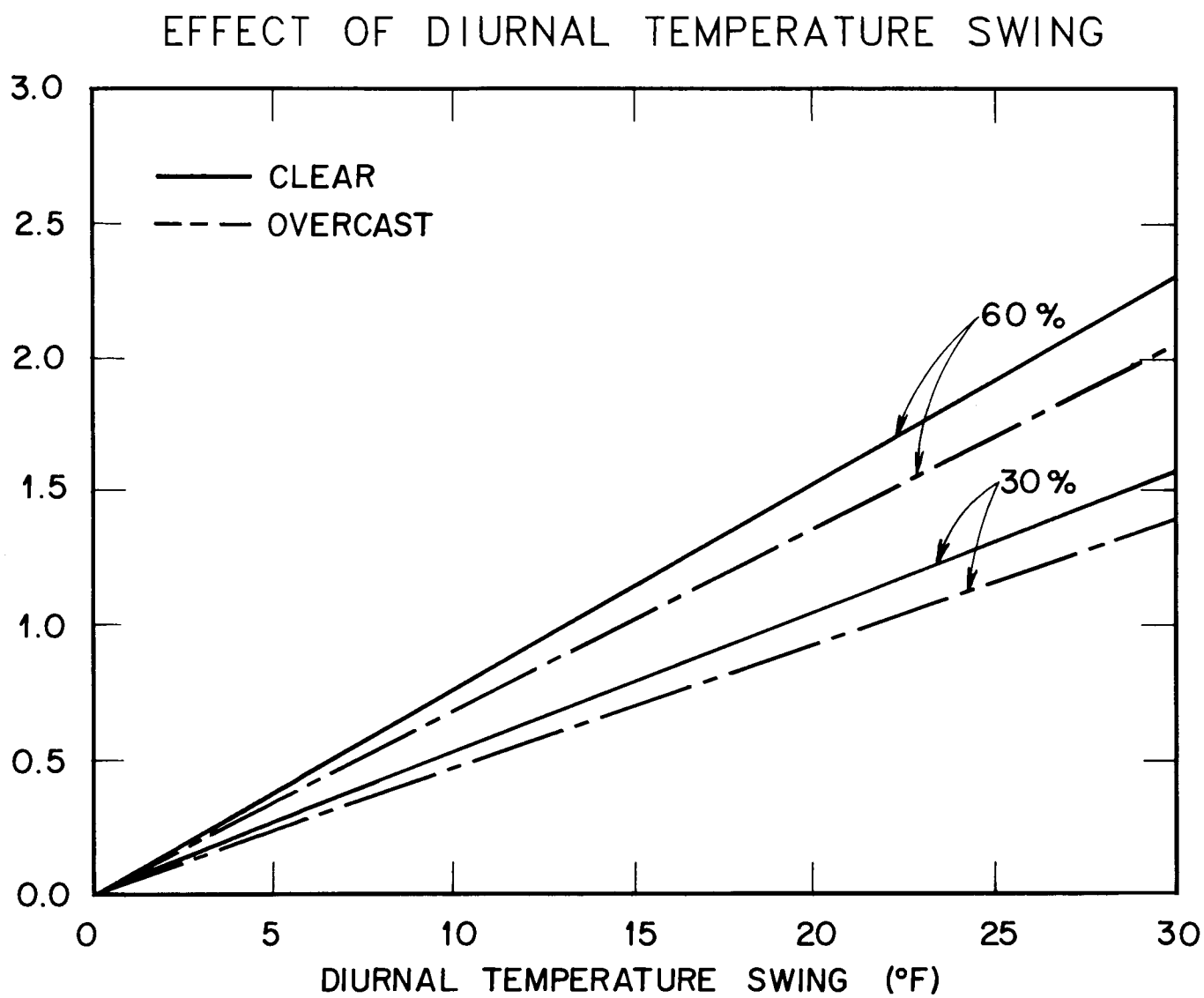

Fig. 12. Effect of diurnal temperature swing on surface ΔT.

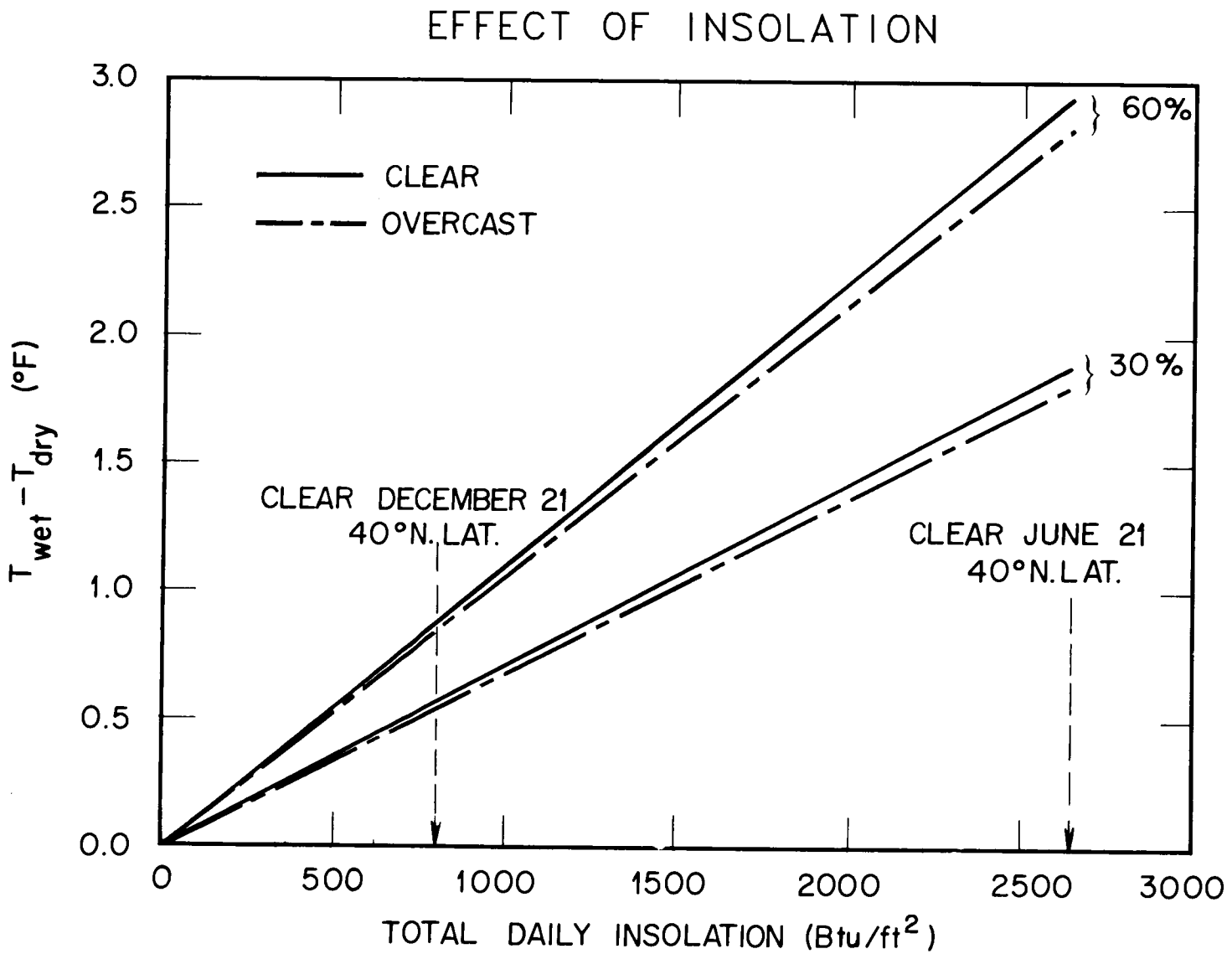

Fig. 13. Effect of insolation on surface ΔT.

ORNL-DWG 83-7427

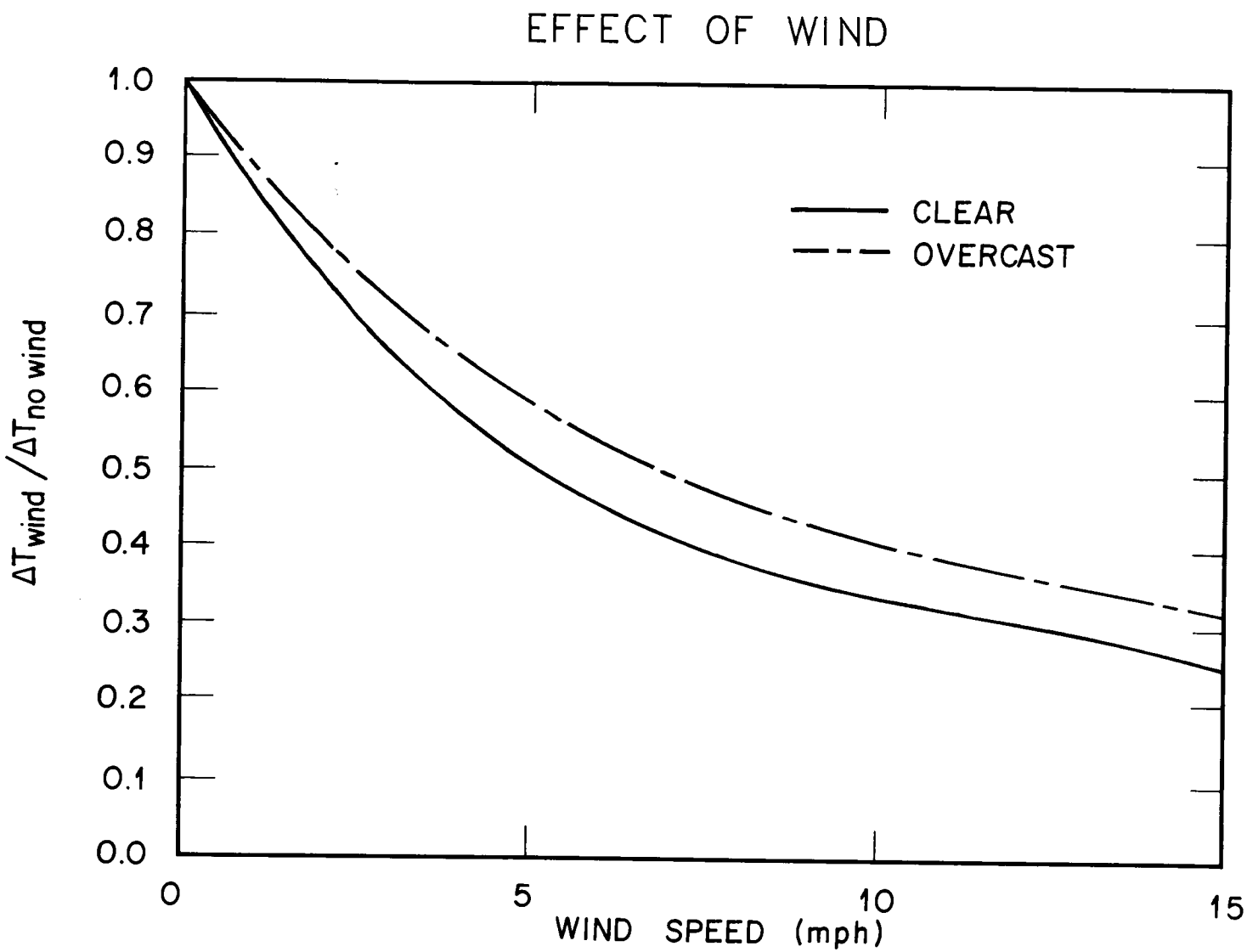

Fig. 14. Effect of wind on surface ΔT.

The individual $\Delta T's$ are obtained from the figures for the particular moisture and sky conditions of interest. This expression gives a quick method of estimating the relative importance of the various parameters and for estimating the net temperature difference for various environmental conditions.

To evaluate the applicability of this simple model, it was checked against the more elaborate numerical model over the range of all of the parameters. The result was that the simple model was always within $\pm 0.8°F$ of the more elaborate model. The simple model overestimates the temperature difference most for cases with a very high moisture content, high average outdoor temperature (above interior), and little or no diurnal swing; but these are poor conditions for observation because the steady-state and dynamic effects cancel each other and produce very small net temperature differences. It underestimates the temperature difference for cases with high moisture content, low average outdoor temperature, and large diurnal swings. However, an error of 0.8°F is not too significant since the temperature differences are large for these cases.

To see how this technique is used, consider a clear midsummer day (2500 Btu/ft^2 insolation), average outdoor temperature of 70°F, a 30°F (55-85°F) diurnal temperature swing, negligible wind, and 30% moisture content (volumetric). For these conditions, the resulting $\Delta T's$ attributable to the average outdoor temperature, diurnal temperature swing, and insolation are, respectively, 1.0°F, 1.6°F, and 1.8°F. Note that the insolation and diurnal swing components (dynamic effects) dominate. This is a typical result for summer viewing.

The resultant ΔT of 4.4°F is readily discernible with conventional imaging equipment, which suggests successful infrared viewing conditions. If cloud cover reduces the insolation to half the clear sky value with a likely reduction in the diurnal temperature swing, say to 20°F, then the ΔT is 1.7°F. This is marginal for reliable interpretation and makes the detection of lesser amounts of moisture questionable. Aside from any interest in this particular example, it is important to note how easy it is to use the curves to arrive at a value for ΔT.

Consider a second example for a midwinter day with 800 Btu/ft^2 insolation for the day, a temperature swing of 20°F, and a daily average of outdoor temperature of 40°F. For these conditions, the resulting $\Delta T's$ attributable to the average outdoor temperature, diurnal temperature swing, and insolation are respectively, 3.8°F, 1.0°F, and 0.6°F. The resulting ΔT is 5.4°F. The average temperature component now clearly dominates. The solar contribution is small, and successful viewing is quite likely independent of any insolation effect.

While Eq. 6 and the accompanying figures are informative as to how the environmental conditions affect the temperature difference between areas of wet and dry insulation on a roof, there are some drawbacks in using them. These results were produced for a specific deck type and insulation level. Also, the fact that only one parameter was varied at a time with the others fixed at nominal values, may result in Eq. 6 not being accurate when applied to cases very far removed from the nominal conditions. To overcome some of these difficulties, another set of runs was performed. In these calculations the parameters were varied collectively rather than individually. Two hundred sets of input data were developed for each case by randomly varying the parameters of interest. The parameters and the range over which they were varied are given in Table 1. In generating the input data, any set that had winter insolation values and summer temperature values was discarded as unrealistic. The sky condition, clear or overcast, refers only to the correlation used to determine the calorimetric sky temperature in the model and is not used to adjust the insolation values. The insolation is dependent only upon the time of year and the latitude. The parameter referred to as fraction of insolation absorbed accounts for the solar absorptivity of the roof and any reduction due to environmental conditions.

Table 1. Parameters and range over which they are varied

Parameter	Minimum	Maximum
Average indoor/outdoor temperature difference	-15.0°F	55.0°F
Diurnal temperature swing	0.0°F	+/-15.0°F
Wind speed	0.0 mph	15.0 mph
Insolation	Dec. 21 values	June 21 values
Fraction of insolation absorbed	0.3	0.9

For a specific roof (4-in. concrete deck, fiberglass insulation, and 60% moisture content), the model was run for all 200 sets of input data assuming clear sky conditions. The results of these runs were used to determine the coefficients in Eq. 7 by using a least-squares fitting technique.

$$\Delta T = (A \cdot \Delta T_{avg} + B \cdot \Delta T_{amp} + C \cdot r \cdot Q_{solar})\, e^{-DV}, \tag{7}$$

where

ΔT_{avg} – average indoor/outdoor temperature difference,
ΔT_{amp} – amplitude of fluctuating component of indoor/outdoor temperature difference,
r – fraction of solar absorbed by roof,
Q_{solar} – maximum solar energy for date and latitude,
V – wind speed.

The form of Eq. 7 is similar to that of Eq. 6. The individual terms in the equation can be interpreted as the temperature difference produced by average indoor/outdoor temperature difference, the temperature difference produced by diurnal temperature swing, the temperature difference produced by solar effects, and the reduction of the temperature difference as a result of the wind. The variation of the coefficients in Eq. 7 with the thickness of the insulation is shown in Fig. 15. Similar plots for different sky conditions, moisture contents, and deck types are given in Figs. 16 through 20.

The indoor/outdoor temperature difference is made up of two components: the average component and a fluctuating component. The coefficients A and B can be interpreted as the temperature difference between areas of wet and dry insulation produced for each 1° change in the average and fluctuating components, respectively. The magnitude of the fluctuating component is one-half of the total diurnal temperature swing. From Figs. 15 through 18 it can be concluded that a 1° diurnal swing produces approximately the same wet/dry temperature difference as a 1° average indoor/outdoor temperature difference.

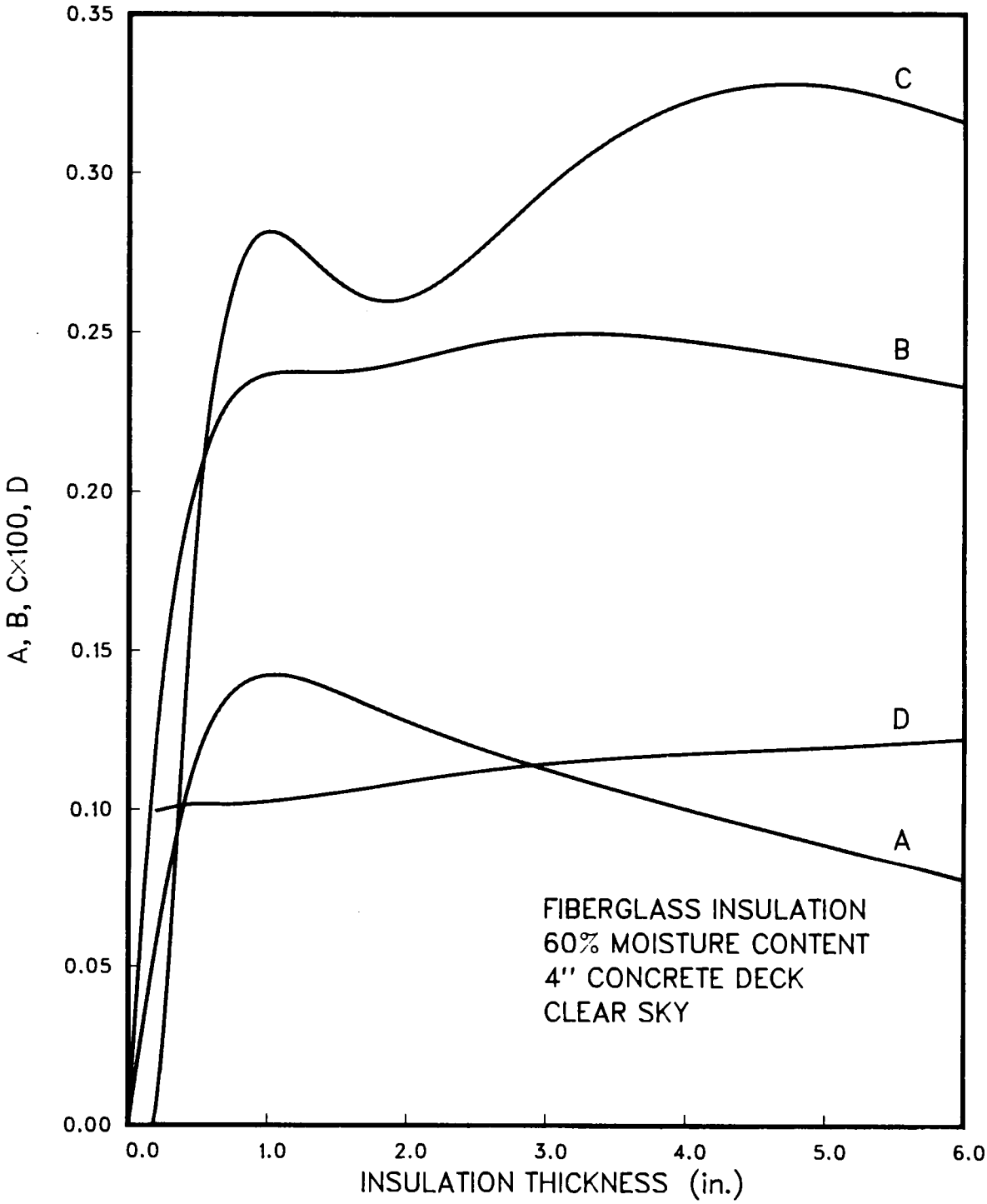

Fig. 15. Coefficients for simple model - case 1.

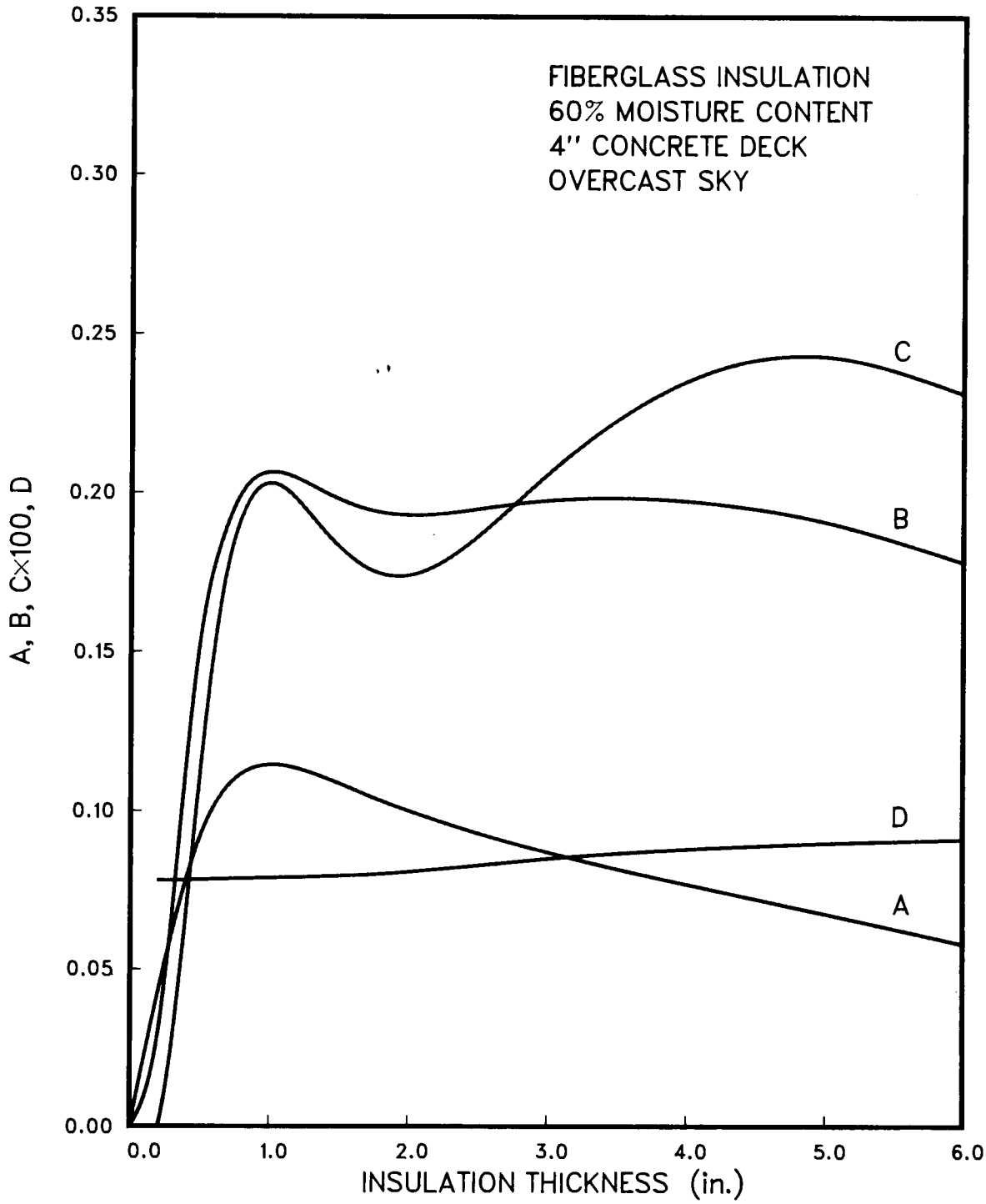

Fig. 16. Coefficients for simple model - case 2.

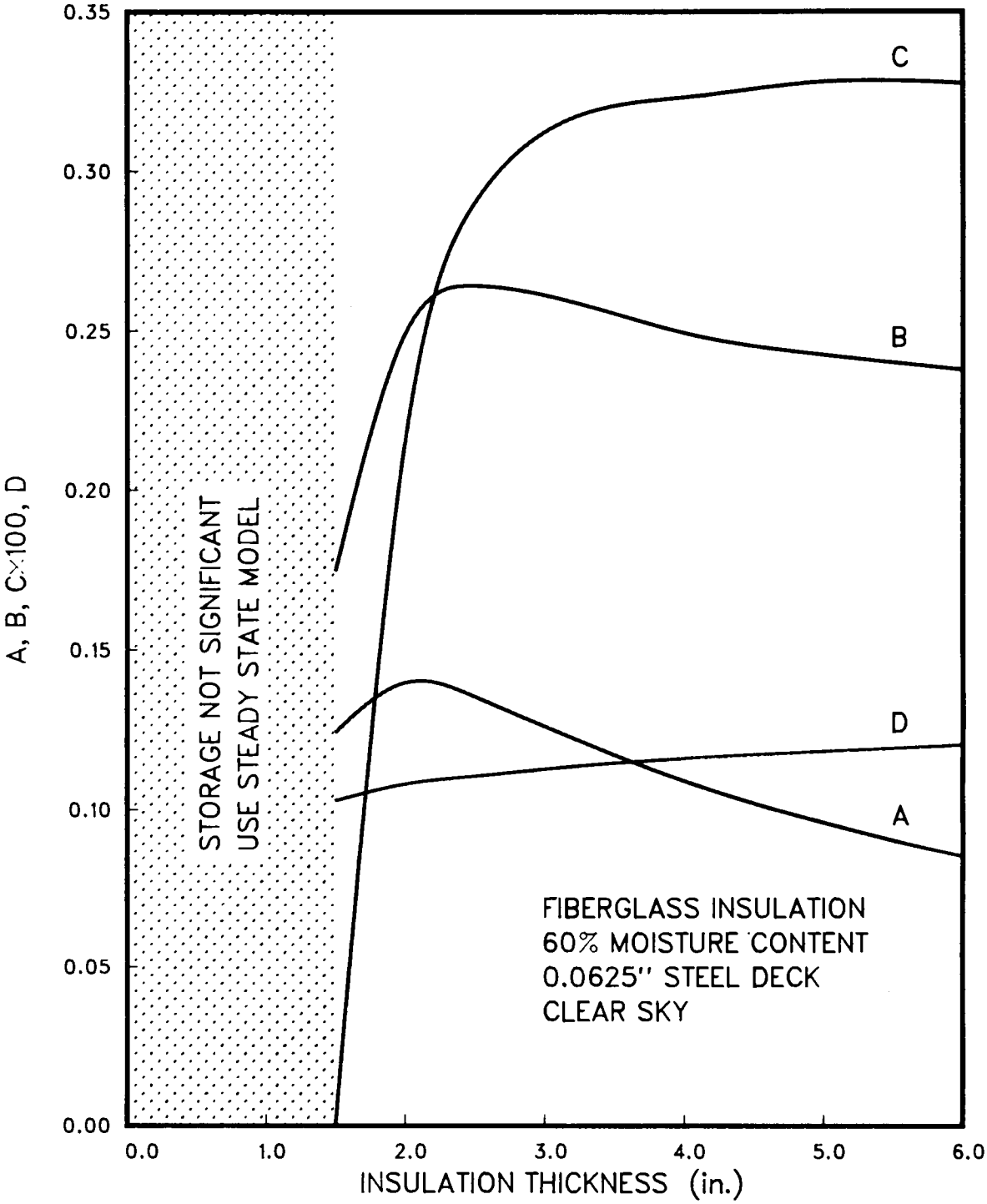

Fig. 17. Coefficients for simple model - case 3.

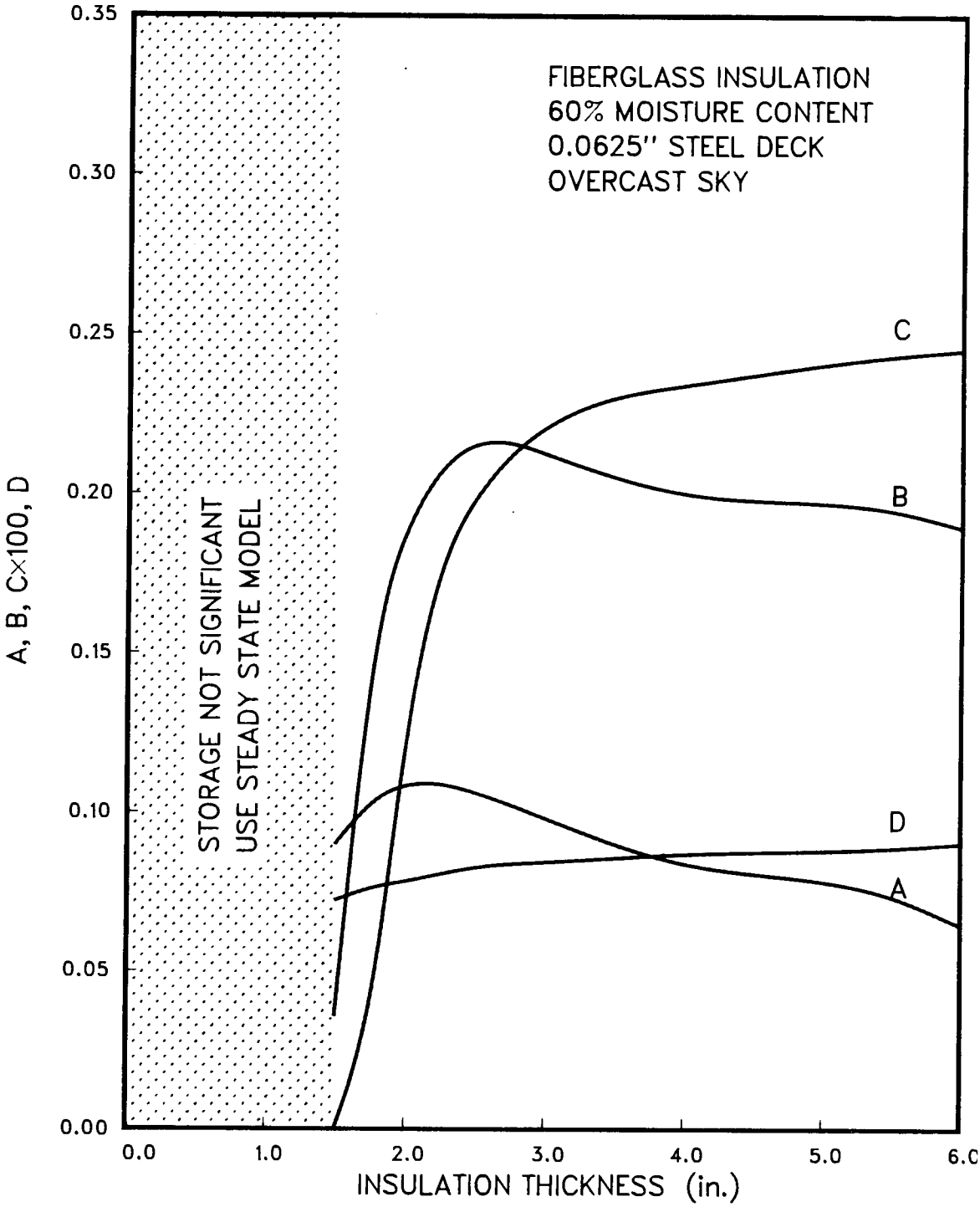

Fig. 18. Coefficients for simple model - case 4.

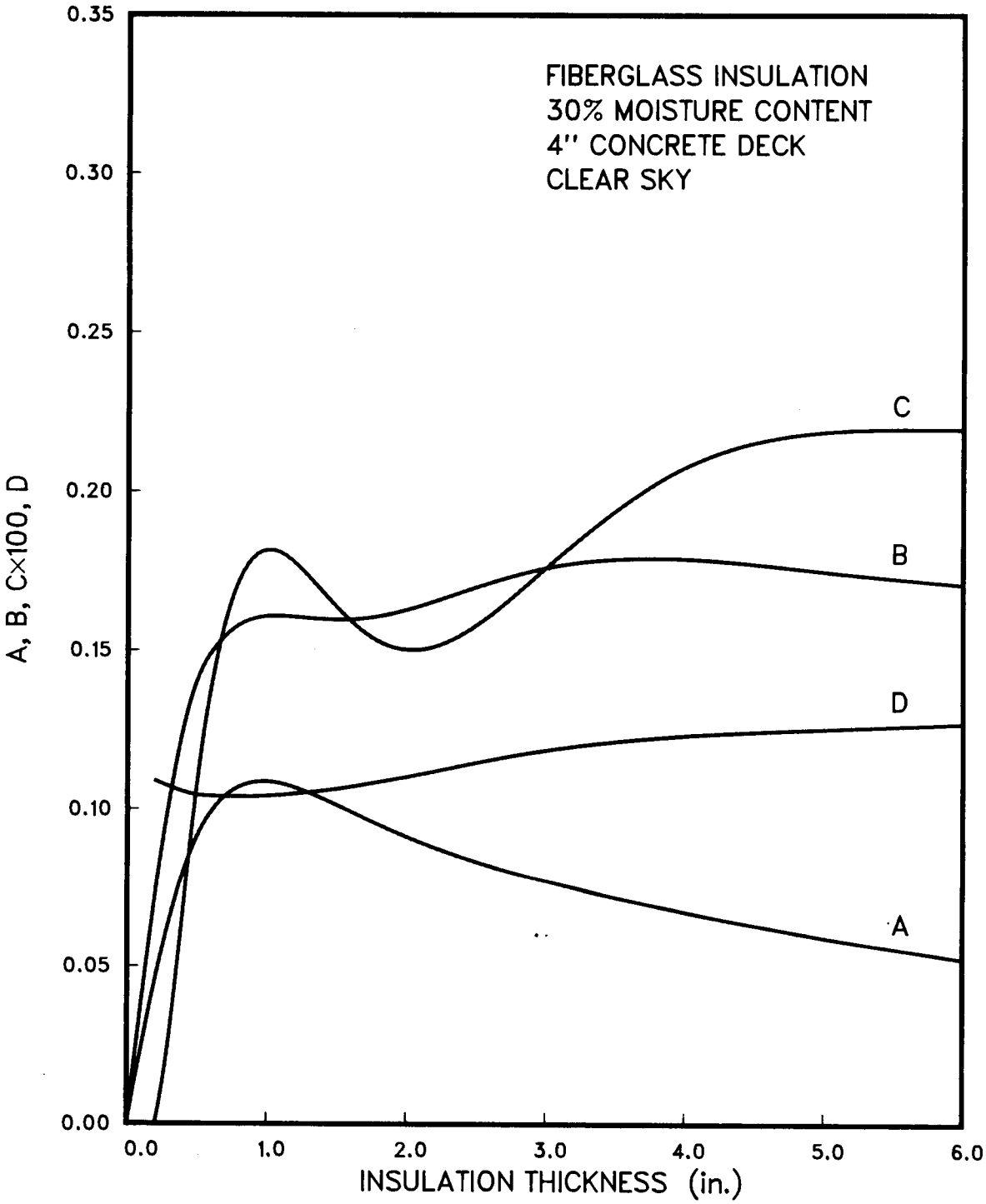

Fig. 19. Coefficients for simple model - case 5.

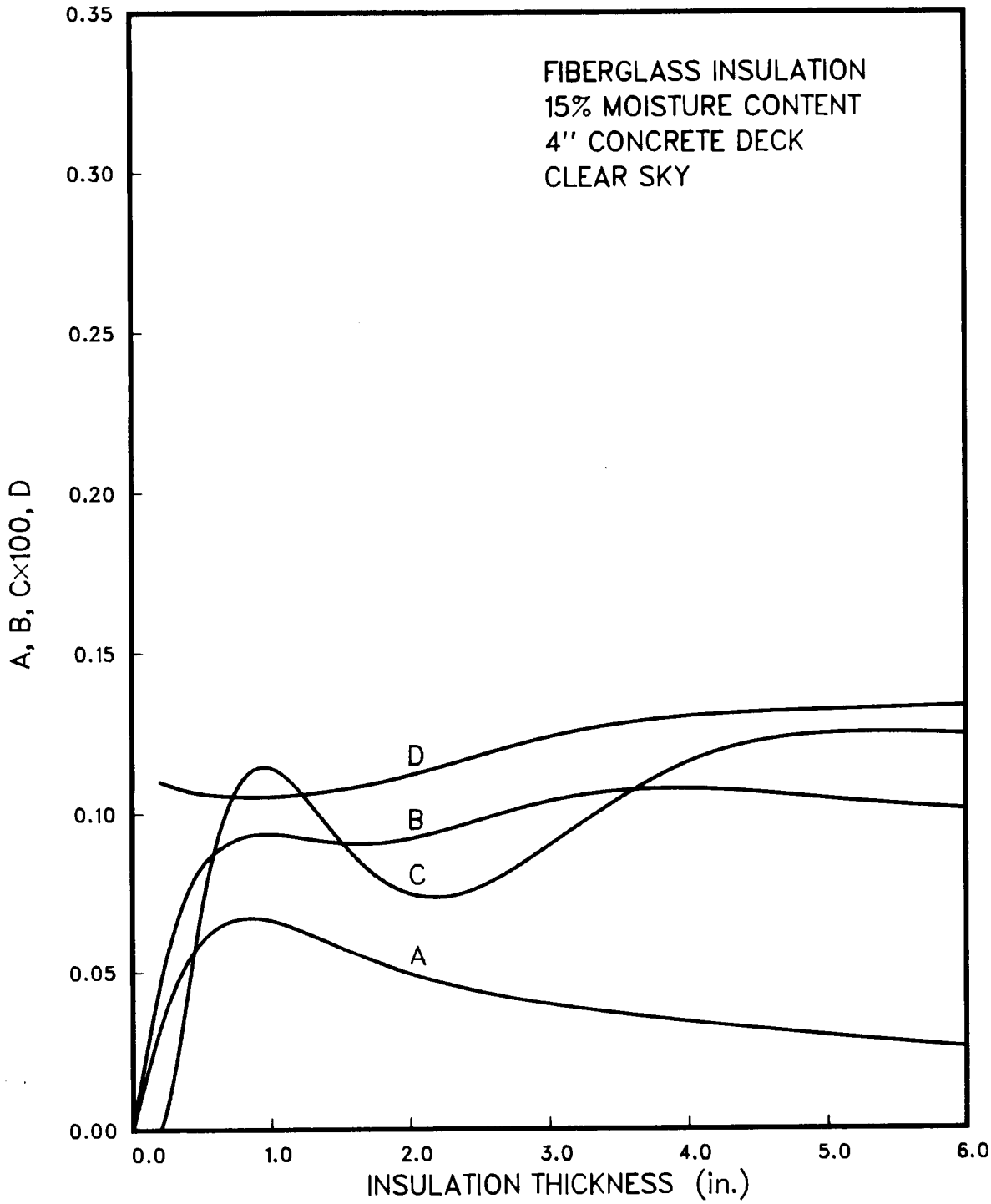

Fig. 20. Coefficients for simple model - case 6.

The coefficient *C* gives an indication of the wet/dry temperature difference resulting from the storage of energy from insolation during the previous day. The coefficient *B* also is related to storage of energy from the previous day when the outside temperature was higher than it was at midnight. In all of the cases with a concrete deck (Figs. 15, 16, 19, and 20), the coefficient *C* (and to a lesser degree, *B*) has a local maximum value at less than 1 in. of insulation and another at a higher insulation level. The cases with a steel deck (Figs. 17 and 18) do not demonstrate the first local maximum in *B* or *C*. This first maximum is due to energy storage in the concrete deck, not in the wet insulation. As the insulation level is increased, the deck becomes more isolated from the outside, and energy storage in the deck becomes less influential on the roof surface temperature. However, for a given volume percent moisture content, the added thickness increases the energy storage capacity of the wet insulation resulting in the second peak in the coefficients.

The steel deck does not have significant energy storage capacity which is why a roof with a steel deck does not have the same behavior at low insulation levels as one with a concrete deck. In fact, the coefficient *C*, which indicates storage of solar energy in the roof, vanishes below insulation levels of approximately 1.5 in. assuming 60% moisture content. At higher insulation levels the behavior of a roof with a steel deck is very similar to that of one with a concrete deck.

By making comparisons between different cases, some general observations can be made about the effect of certain parameters. For example, coefficient *D*, which indicates the influence of the wind on the wet/dry temperature difference, is not significantly affected by moisture content, insulation thickness, or deck type. It is, however, affected by the sky condition. An overcast sky significantly decreases the observed wet/dry temperature difference, as does decreasing moisture content in the insulation.

Figure 21 presents the temperature difference predicted by the simple model plotted against that predicted by the computer model for a case with 60% moisture content, fiberglass insulation, 4-in. concrete deck, and clear sky. Each data point on the plot represents the results for a given set of conditions. The abscissa of each point is the temperature difference predicted by the computer model, and the ordinate is the temperature difference predicted by the simple model for the same conditions. If both models predict the same temperature difference, the data point will fall on the diagonal line shown on the figure. The farther a data point falls from the diagonal, the greater the discrepancy between the simple model and the computer model. To avoid excessive clutter on the plot, only 100 of the 200 runs for this case are presented. The results show a reasonable match between the simple model and the computer model. These results are typical of what was observed for the other cases.

INFLUENCE OF OTHER FACTORS

There are several other factors that influence the wet/dry temperature difference on a roof surface. Some of these are addressed in this section: insulation type, moisture distribution within the insulation, gravel thickness, and viewing time.

Since the presence of water does not have the same effect on all types of insulation, the results presented in this report may not be valid for other insulation types. To get some feel for the importance of insulation type, a set of runs was done using expanded polystyrene insulation (EPS). EPS was chosen because its characteristics are so different from glass fiberboard. A plot of the *A*, *B*, *C*, and *D* coefficients for Eq. 7 are plotted in Fig. 22 as a function of insulation thickness. The results presented in this figure are directly comparable to those in Fig. 19 since they differ only in the insulation type. The coefficients for these two cases are very similar. The coefficients *B* and *D* are almost identical for the two cases. The *A* coefficient is slightly lower for EPS at all insulation

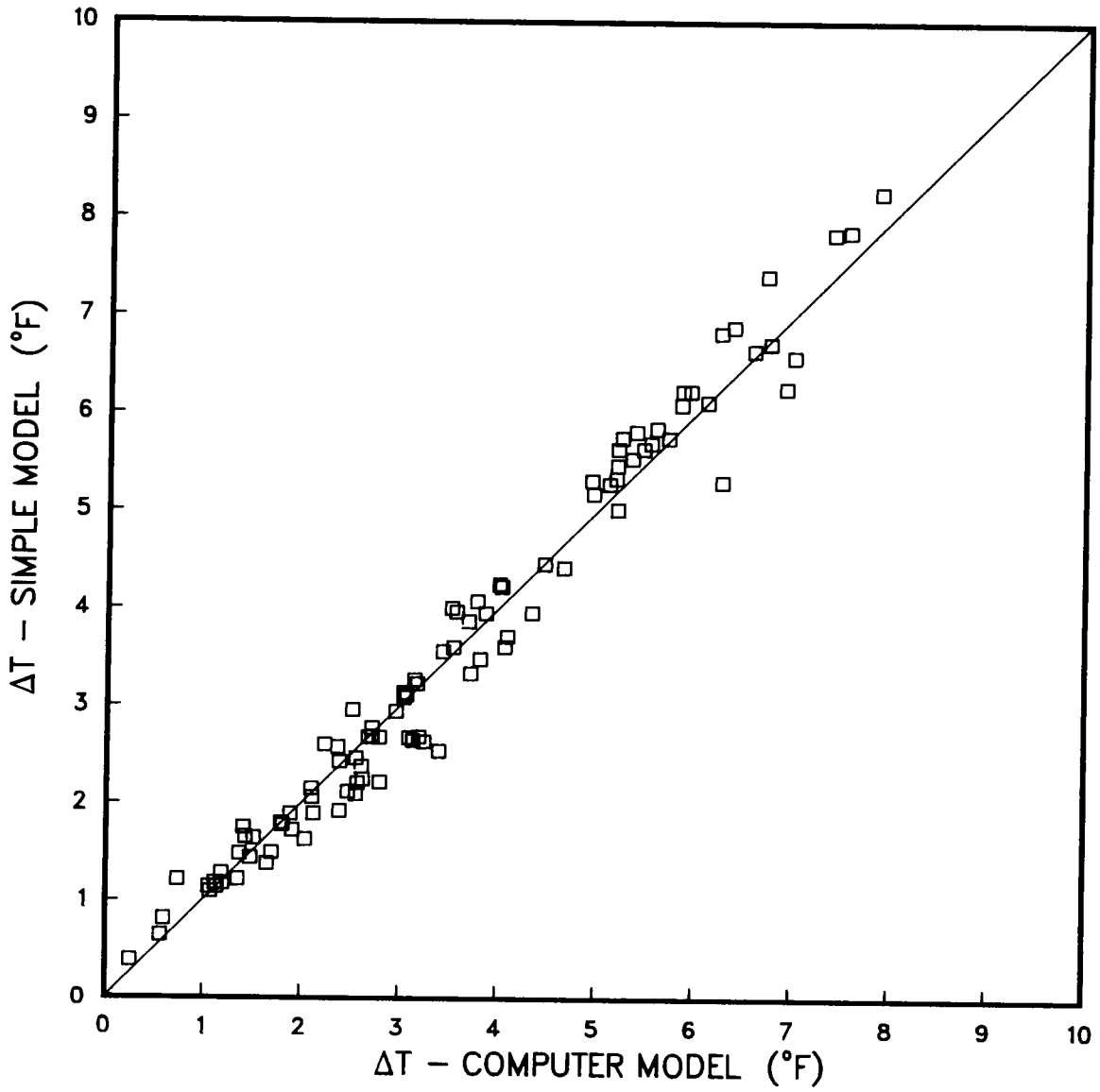

Fig. 21. Comparison of simple model and computer model results.

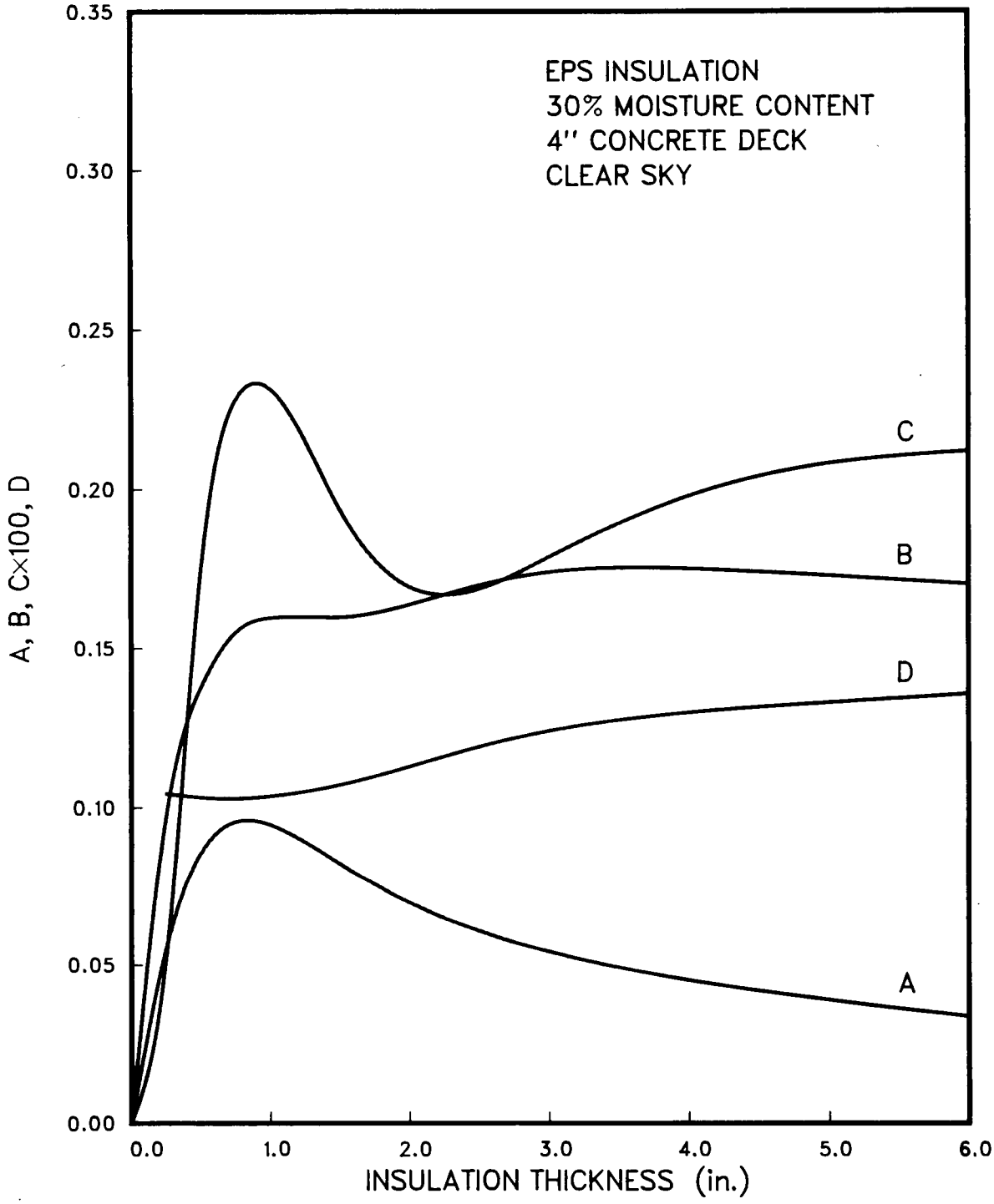

Fig. 22. Coefficients for simple model - case 7.

thicknesses; but, considering the large difference in R value-per-inch for these two insulations, the values are remarkably close. The peak in the *C* coefficient at about 1 in. of insulation is higher for EPS than for fiberglass, but at higher insulation levels the values are very close. For general guidelines, the information presented in this report for glass fiber insulation may be of use for other insulation types.

It was assumed in the development of the results reported here that the moisture was uniformly distributed throughout the thickness of the insulation. In practice, thick insulation is often made up of several layers of insulation board. There often is even a membrane on one surface of the individual insulation boards that is impervious to water. Thus, it is conceivable that the moisture is not uniformly distributed. A likely arrangement would be that, due to gravity, the lower portion of the insulation may contain moisture while the upper portion remains dry. To see what effect this would have, a case was run in which the lower half of the insulation contained 60% moisture by volume and the upper half was dry. The *A*, *B*, *C*, and *D* coefficients are plotted as a function of thickness (Fig. 23). The total amount of water in the insulation in this case is the same as if there were 30% moisture by volume distributed uniformly through the insulation. A comparison of the current results with those for 30% uniformly distributed moisture (Fig. 19) shows that the *A*, *B*, and *C* coefficients (i.e., the ones indicating the effects that produce the observed wet/dry temperature difference) are all dramatically lower when the wet insulation is in the lower half. The *D* coefficient is approximately the same for both cases.

To further demonstrate the effects of moisture location, a series of runs was performed in which the moisture was placed in the upper half only, the lower half only, or uniformly distributed. These cases were run with 2 in. of fiberglass insulation and hypothetical winter conditions. The resulting wet/dry roof surface temperature differences versus moisture content as a percent of the total volume of the insulation (not just the wet insulation volume) are presented in Fig. 24. Moisture concentrated in the upper half, or uniformly distributed, can be much more easily detected on the basis of surface temperature than can moisture concentrated in the lower half of the insulation.

All of the calculations were performed with ½ in. of gravel topping on the roof. If there are more gravel than this on the roof it could affect the wet/dry temperature difference. The additional gravel adds considerable heat capacity to the roof and some insulating value, thus isolating the insulation somewhat from the outside environment. Figure 25 shows the effect of additional gravel on observed wet/dry roof surface temperatures for both winter and summer conditions. Another problem that may be encountered is the uneven distribution of gravel thickness across a roof. This in itself could produce temperature differences which would make interpretation of infrared results difficult.

All of the results presented in this report are for a viewing time of midnight. The effect of viewing time on the observed wet/dry temperature difference was investigated for representative winter and summer conditions. The results are presented in Fig. 26. In the winter the temperature difference increases throughout the night. Early morning hours would be slightly better for observing temperature differences than midnight. For the summer conditions, the temperature difference is relatively constant throughout the night.

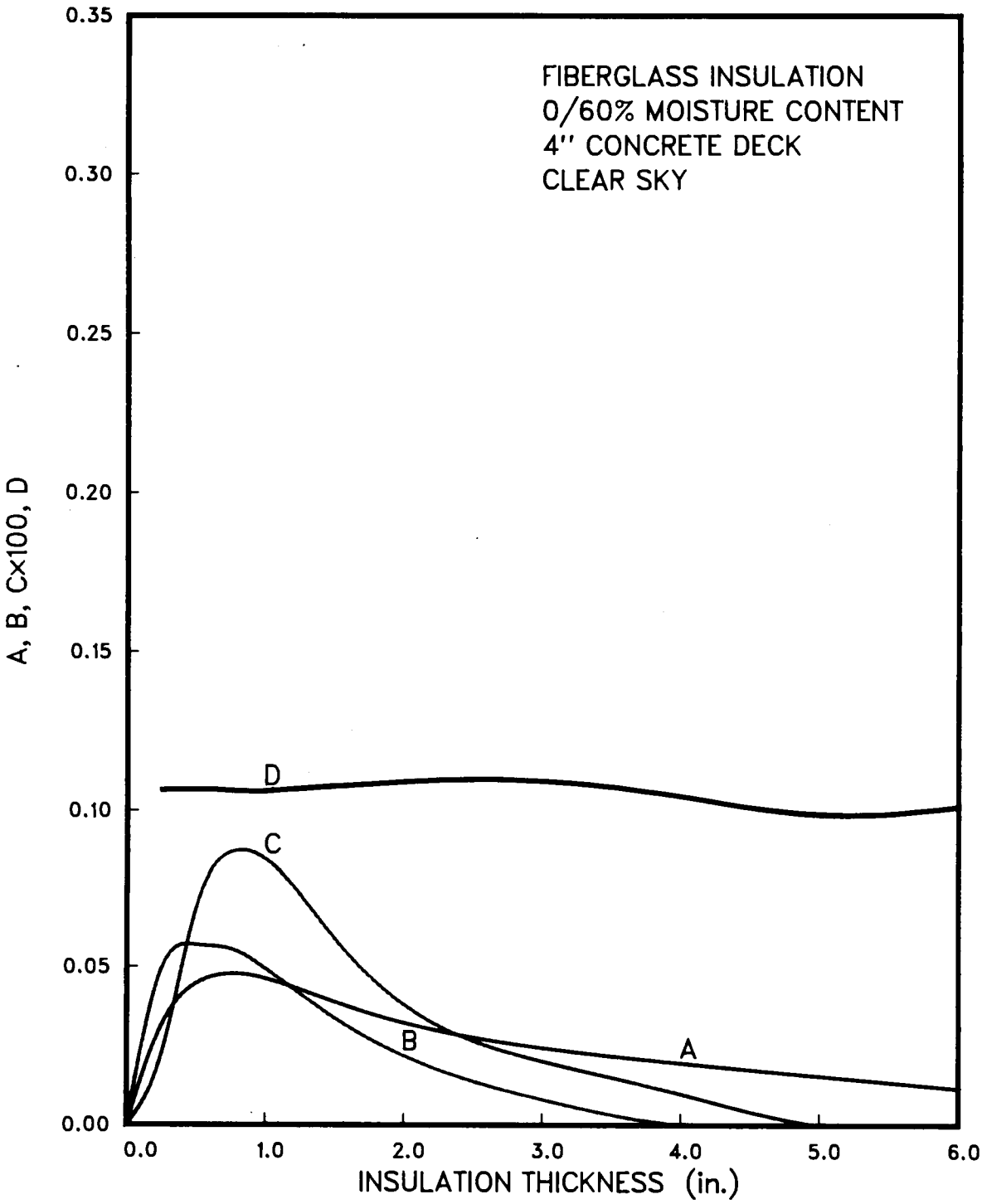

Fig. 23. Coefficients for simple model - case 8.

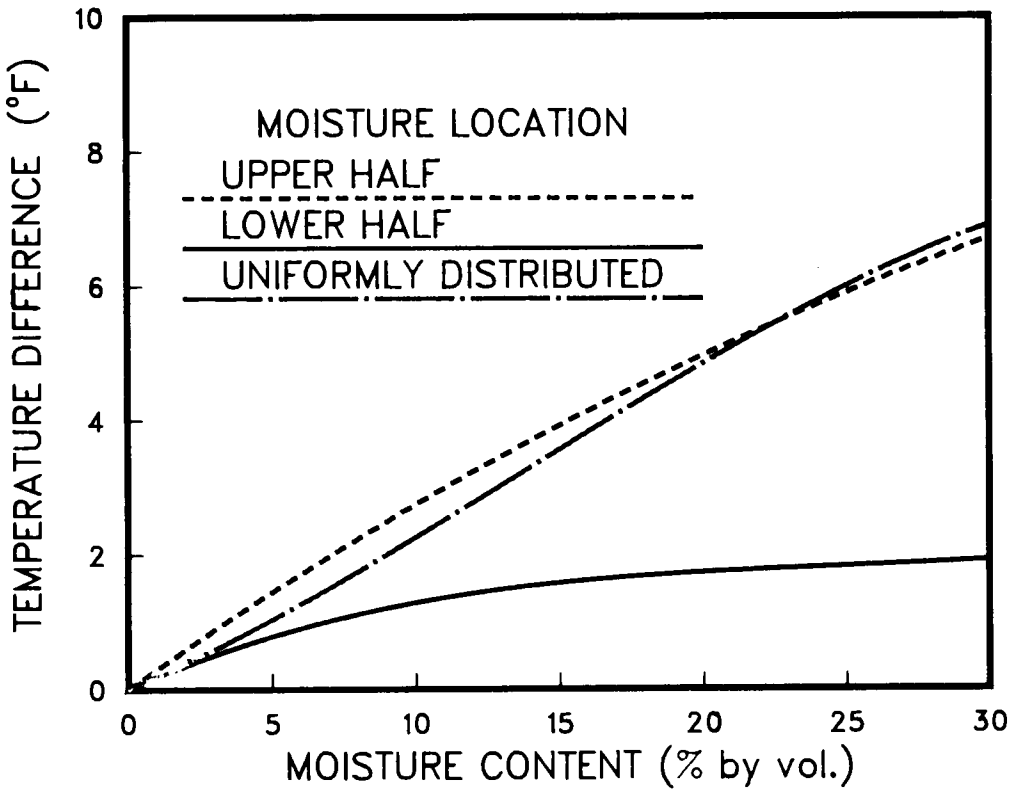

Fig. 24. Effect of moisture location on wet/dry temperature difference.

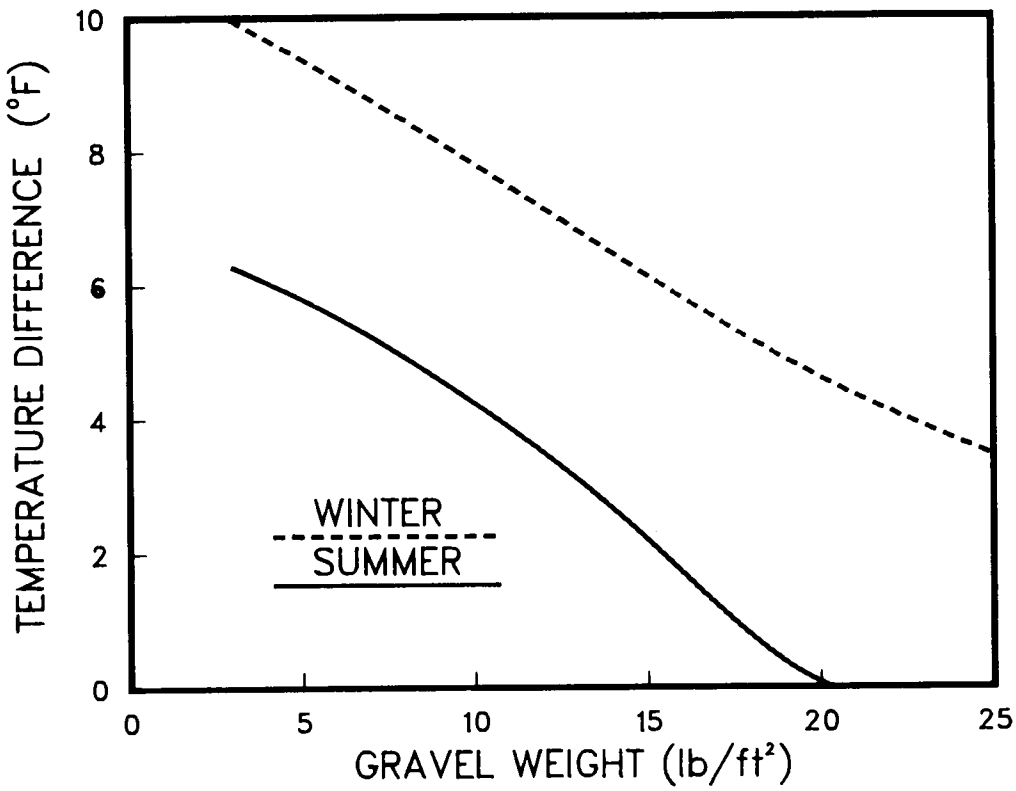

Fig. 25. Effect of gravel weight on wet/dry temperature difference.

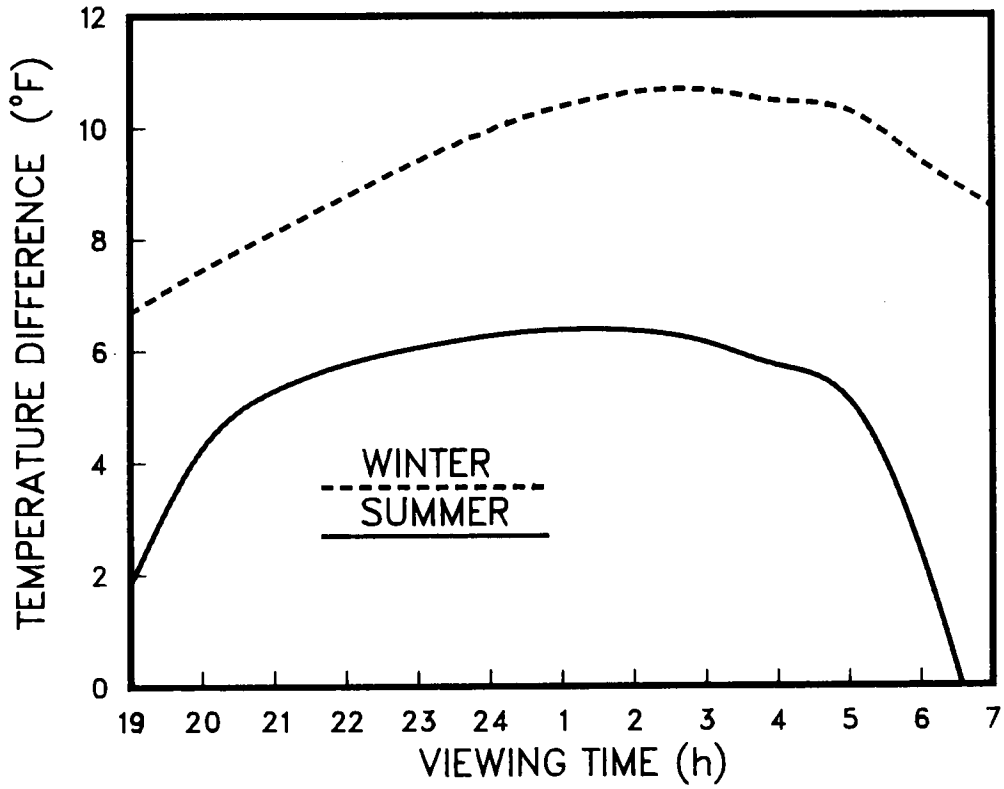

Fig. 26. Effect of viewing time on wet/dry temperature difference.

CONCLUSIONS AND RECOMMENDATIONS

The results presented in this report can be used as general guidelines for judging the relative importance of various factors on the roof surface temperature difference between areas containing wet insulation and those containing dry insulation. However, they should not be taken as an accurate prediction of the actual wet/dry temperature difference on a particular roof for certain environmental conditions. The "simple" model developed from the numerical model is still somewhat cumbersome to use and is not applicable to all roof types and environmental conditions. An easier-to-use model may still be needed, and it could perhaps be developed; however, it is not recommended that this be pursued at the present time. The numerical model handles the moisture in a rather simplistic manner and has not been verified against experimental results with moisture in the insulation. Further modeling efforts should await results from experiments being conducted at the RTRA facility on the effect of moisture.

ACKNOWLEDGMENTS

The work presented in this report was done as a part of the National Program for Building Envelope Systems and Materials. The research was sponsored by the Office of Buildings and Community Systems, Building Division, U. S. Department of Energy. Special appreciation is extended to L. W. Winborn who prepared this report for publication.

REFERENCES

1. J. R. Jack and R. L. Bowman, *Reliable Aerial Thermography for Energy Conservation*, DOE/NASA/20270-1, NASA TM-81766, U.S. DOE, Div. Building and Community Systems, August 1981.
2. D. M. Burch, "Infrared Audits of Roof Heat Loss," *ASHRAE Transactions*, vol. 86 (Pt 2), 1980.
3. R. J. Goldstein, "Application of Aerial Infrared Thermography," *ASHRAE Transactions*, vol. 84, (Pt 1), 1978.
4. A. H. Knehans and P. E. Styer, "Thermography - A Diagnostic Tool for Locating Wet Insulation in Built-Up Roofs," *Thermal Infrared Sensing Diagnostic (Thermosense V)*, George E. Courville, Editor, Proc. SPIE 371, pp. 164-167 (1982).
5. C. Korhonen and W. Tobiasson, "Locating Wet Cellular Plastic Insulation in Recently Constructed Roofs," *Thermal Infrared Sensing Diagnostic (Thermosense V)*, George E. Courville, Editor, Proc SPIE 371, pp. 168-173 (1982).
6. D. C. Fishburn, "Comparing the Effectiveness of Ground Versus Aerial Roof Thermography," *Thermal Infrared Sensing Diagnostics (Thermosense V)*, George E. Courville, Editor, Proc SPIE 371, pp. 177-186 (1982).
7. W. Tobiasson, "Roof Moisture Surveys: Current State of the Technology," *Thermal Infrared Sensing Diagnostics (Thermosense V)*, George E. Courville, Editor, Proc. SPIE 371, pp. 24-31 (1982).
8. W. C. Swinbank, "Long-Wave Radiation from Clear Skies," Quart. *J. R. Meterol Soc.*,vol. 89, No. 381, pp. 339-348 (July 1963).
9. R. W. Bliss, "Atmospheric Radiation Near the Surface of the Ground: A Summary for Engineers," *Solar Energy*, vol. 5, pp. 103-120 (1961).
10. R. J. Goldstein, an unpublished study as reported by J. R. Jack and R. L. Bowman, "Reliable Aerial Thermography for Energy Conservation," DOE/NASA/20270-1, NASA TM-81766, U.S. DOE, Div. Building and Community Systems, August 1981.
11. *ASHRAE Handbook of Fundamentals*, American Society of Heating, Refrigerating, and Air Conditioning Engineers, Inc., New York, 1977.

INTERNAL DISTRIBUTION

1. C. B. Bryan
2. R. S. Carlsmith
3. K. W. Childs
4. J. E. Christian
5. J. S. Crowell/G. E. Whitesides
6. W. Fulkerson
7. T. S. Lundy
8-22. M. C. Matthews
23. H. McLain
24. J. W. Michel
25. W. R. Mixon
26-28. D. S. Napolitan
29. J. P. Sanders
30. J. N. Tunstall
31. L. W. Winborn
32. Central Research Library
33. Document Reference Section, Y-12
34-36. Enrichment Technology Library
37-39. Laboratory Records
40. ORGDP Plant Records (RC)
41. ORNL Patent Office
42. Central Research Library
43. Document Reference Section

EXTERNAL DISTRIBUTION

44. R. L. Alumbaugh, Naval Civil Engineering Lab., Port Hueneme, Calif.
45. C. G. Bankvall, Swedish National Testing Institute, Boras, Sweden
46. S. M. Benner, Drexel University, Philadelphia, Pa.
47. J. J. Boulin, Dept. of Energy, Buildings Division, Washington, D.C.
48. H. W. Busching, Clemson University, Clemson, S.C.
49. J. H. Cable, John Cable Associates, Inc., Alexandria, Va.
50. W. R. Goss, University of Massachusetts, Amherst, Mass.
51. F. A. Govan, ZBA, Inc., Cincinnati, Ohio
52. E. I. Griggs, Tennessee Technological University, Cookeville, Tenn.
53. R. A. Grot, National Bureau of Standards, Gaithersburg, Md.
54. C. Guilford, Bothell, Wash.
55. J. Klems, Lawrence Berkeley Laboratory, Berkeley, Calif.
56. R. H. Kolodin, Office of Public Housing & Urban Development, Washington, D.C.
57. W. M. Kroner, Rensselaer Polytechnic Institute, Troy, N.Y.
58. R. A. LaCosse, National Roofing Contractors Association, Oak Park, Ill.
59. E. Leger, New Ipswich, N.H.
60. D. R. McCullough, Urethane Foam Contractors Association, Austin, Tex.
61. D. McGuire, Regal Industries, Crothersville, Ind.
62. M. Milne, University of California, Los Angeles, Calif.
63. M. P. Modera, Lawrence Berkeley Laboratory, Berkeley, Calif.
64. P. G. Mulroney, VVKR, Inc., Alexandria, Va.
65. R. Orlandi, W. R. Grace & Company, Cambridge, Mass.
66. D. E. Richards, Owens Corning, Commercial Roofing Division, Toledo, Ohio
67. J. N. Rogers, Div. 8324, Sandia Laboratories, Livermore, Calif.
68. W. J. Rossiter, National Bureau of Standards, Gaithersburg, Md.
69. J. Samos, NASA, Hampton, Va.
70. S. Selkowitz, Lawrence Berkeley Laboratory, Berkeley, Calif.

EXTERNAL DISTRIBUTION (cont.)

71-72. M. Sherman, Jim Walter Corporation, St. Petersburg, Fla.
73. C. J. Shirtliffe, National Research Council of Canada, Ottawa, Canada
74. S. E. Smith, Dynatech R/D Co., Cambridge, Mass.
75. L. G. Spielvogel, Wyncote House, Wyncote, Pa.
76. R. Sterling, University of Minnesota, Minneapolis, Minn.
77. T. W. Tong, University of Kentucky, Lexington, Ky.
78. G. A. Tsongas, Portland State University, Portland, Oreg.
79. R. P. Tye, Dynatech R/D Co., Cambridge, Mass.
80. M. G. Van Geem, Portland Cement Association, Skokie, Ill.
81. C. R. Vander Linden, Manville Corporation, Denver, Colo.
82. J. R. Warner, ACEC Research and Management Foundation, Washington, D.C.
83. D. W. Yarbrough, Tennessee Technological University, Cookeville, Tenn.
84. Division of Engineering, Mathematics and Geosciences, DOE, Washington, D.C.
85. Office of Assistant Mgr. for Energy Research and Development, Oak Ridge, Tenn.
86-115. Office of Scientific and Technical Information, Oak Ridge, Tenn.